SHOCKS AND ENERGETIC PARTICLES
Sun – Wind – Planets – Heliosphere

Heliophysics Summer School 2013

David Burgess
Astronomy Unit
Queen Mary University of London

With thanks to Manfred Scholer

OUTLINE

- Why shocks?
- Shocks in the solar system
- Some shock physics
  - MHD conservation relations
  - MHD discontinuities
  - Shock parameters
  - Structure of collisionless shocks
- Observations of energetic particles
- Particle acceleration at shocks
  - Shock drift acceleration
  - Diffusive shock acceleration
- Modelling interplanetary energetic particles

Object in supersonic flow – Why a shock is needed

If flow sub-sonic information about object can transmitted via sound waves against flow

Flow can respond to the information and is deflected around obstacle in a laminar fashion

If flow super-sonic signals get swept downstream and cannot inform upstream flow
about presence of object

A shock is launched which stands in upstream flow and effects a super- to sub-sonic
transition

The sub-sonic flow behind the shock is then capable of being deflected around the object

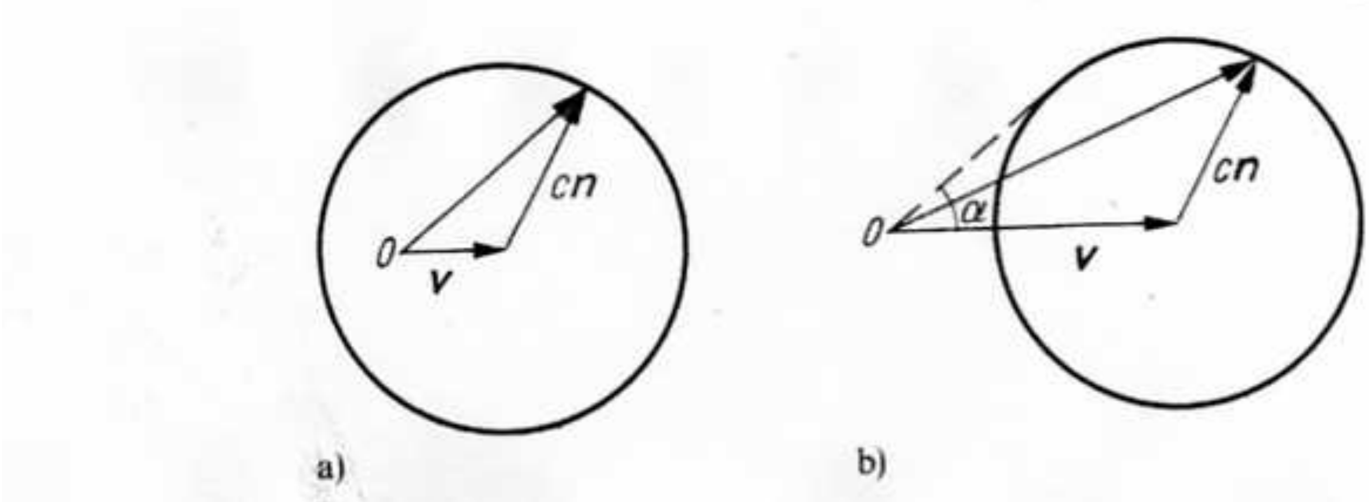

Fluid moves with velocity **v**; a disturbance occurs at 0 and propagates with velocity of sound c relative to the fluid

The velocity of the disturbance relative to 0 is **v** + c **n,** where **n** is unit vector in any direction

(a) v<c : a disturbance from any point in a sub-sonic flow eventually reaches any point
(b) v>c: a disturbance from position 0 can reach only the area within a cone given by opening angle 2α, where $\sin\alpha = c / v$

Surface a disturbance can reach is called Mach's surface

Ernst Mach

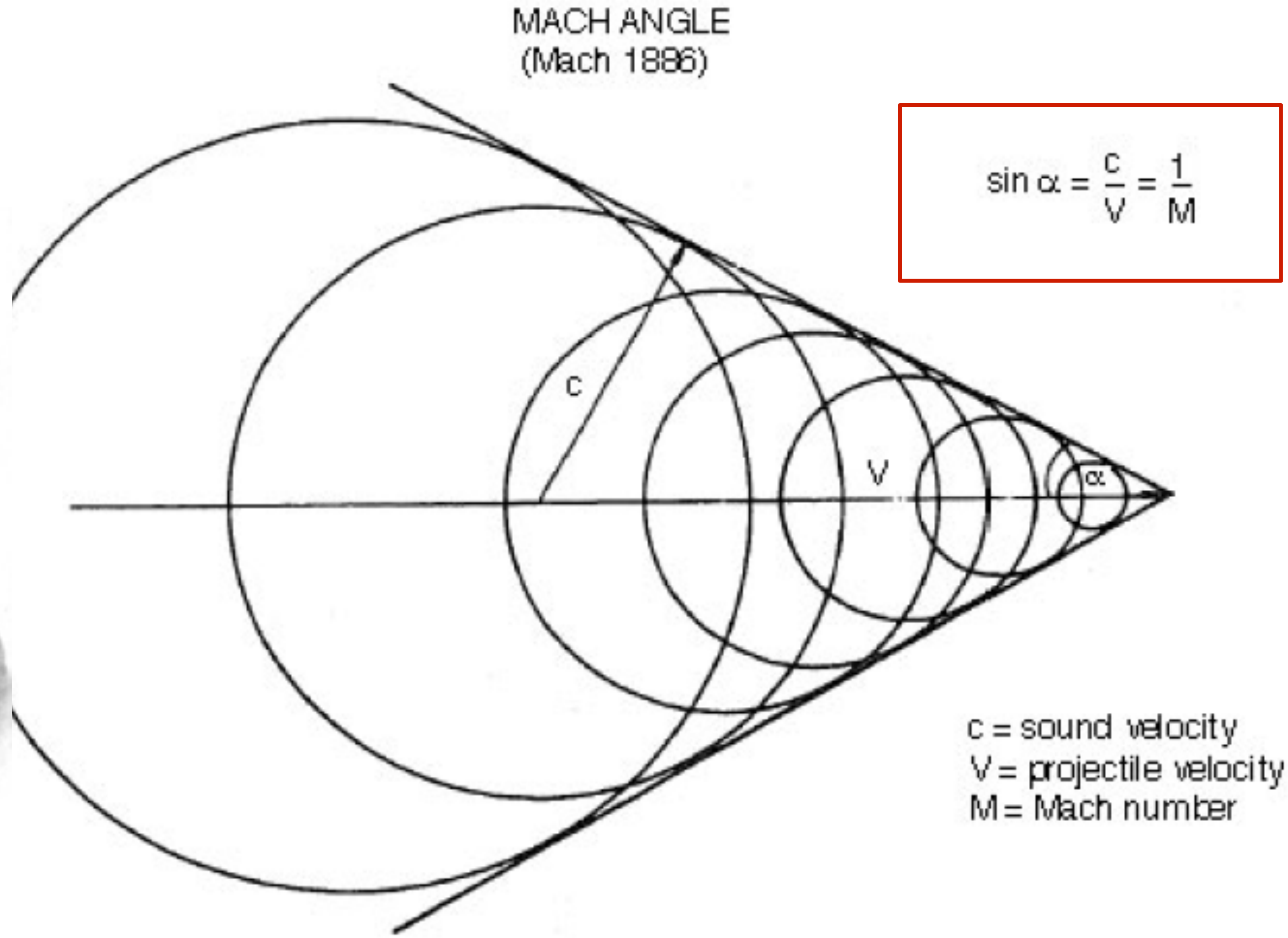

MACH ANGLE
(Mach 1886)
sin α = c/V = 1/M
c
V
α
c = sound velocity
V = projectile velocity
M = Mach number

Examples of a Gasdynamic Shock

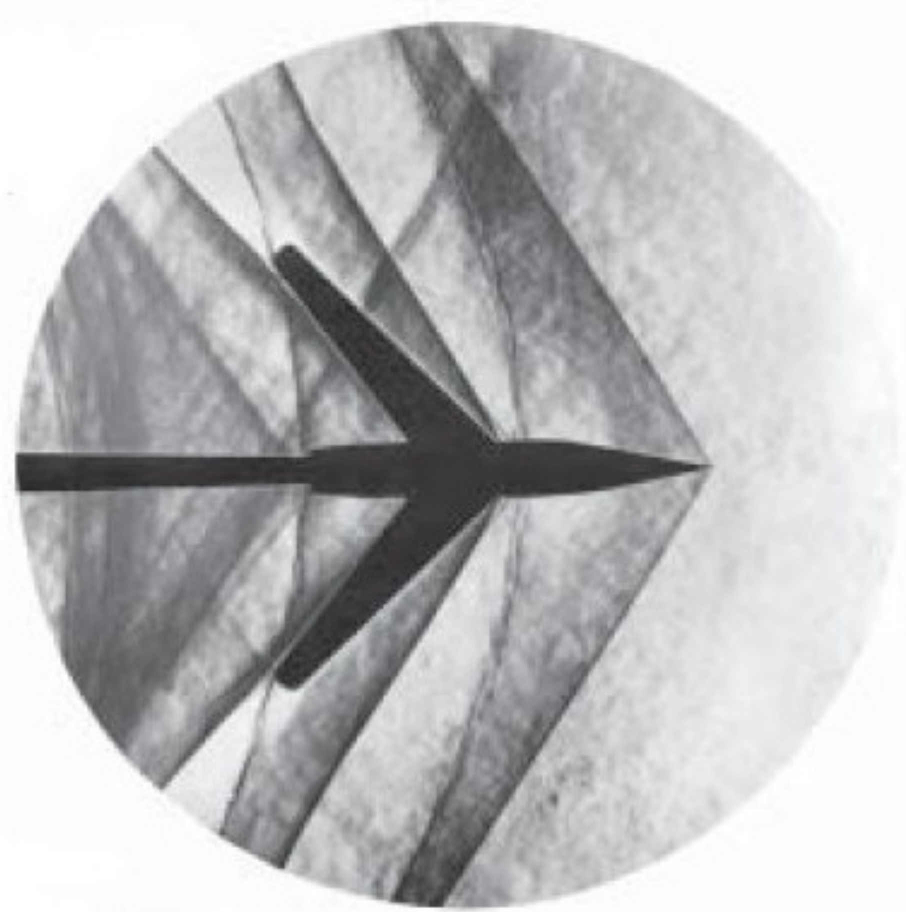

'Schlieren' photography

More Examples

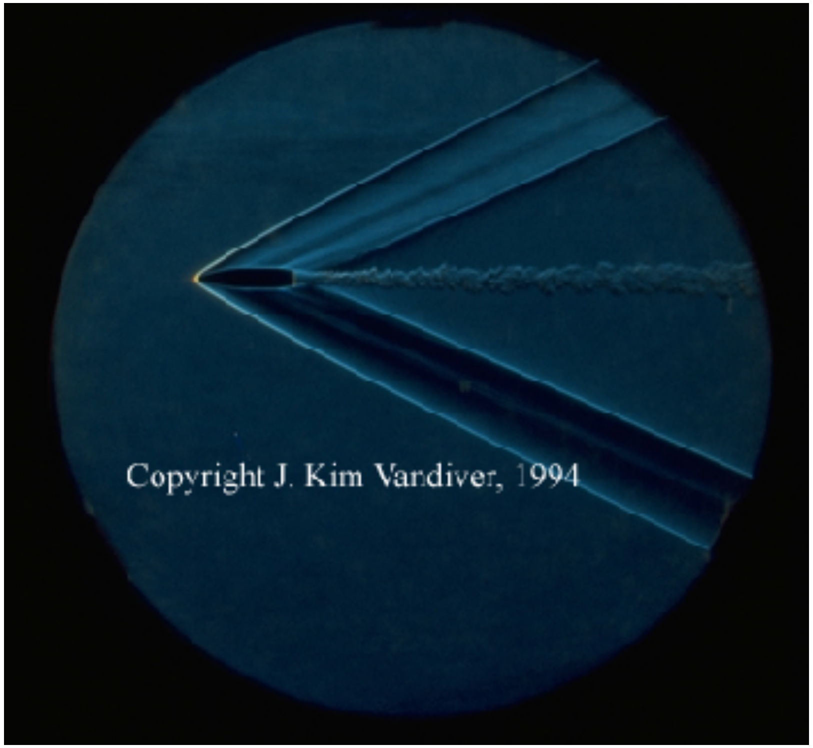

Shock attached to a bullet

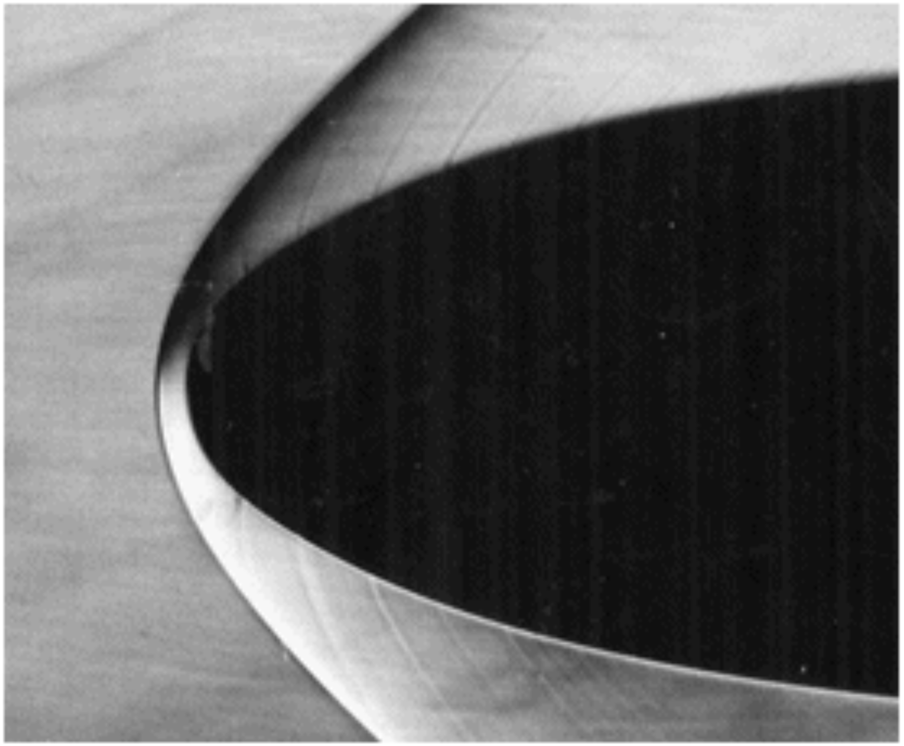

Shock around a blunt object: detached from the object

SHOCKS IN SOLAR SYSTEM

Plasma collisionless, but MHD description still useful
MHD wave modes: fast, slow and Alfven

Solar wind flow: 300-700 km/s
Alfven speed: 50 km/s

Impulsive events: Flares, CME
Obstacles: planets – magnetospheres, ionospheres

There *HAVE* to be shocks!

Historical Note on Plasma Shocks

PHYSICAL REVIEW VOLUME 80, NUMBER 4 NOVEMBER 15, 1950

Magneto-Hydrodynamic Shocks*

F. DE HOFFMANN AND E. TELLER
Los Alamos Scientific Laboratory, Los Alamos, New Mexico

(Received July 10, 1950)

A mathematical treatment of the coupled motion of hydrodynamic flow and electromagnetic fields is given. Two simplifying assumptions are introduced: first, the conductivity of the medium is infinite, and second, the motion is described by a plane shock wave. Various orientations of the plane of the shock and the magnetic field are discussed separately, and the extreme relativistic and unrelativistic behavior is examined. Special consideration is given to the behavior of weak shocks, that is, of sound waves. It is interesting to note that the waves degenerate into common sound waves and into common electromagnetic waves in the extreme cases of very weak and very strong magnetic fields.

Frederic De Hoffmann [& Wife];Edward Teller [& Wife]

Interplanetary traveling shocks

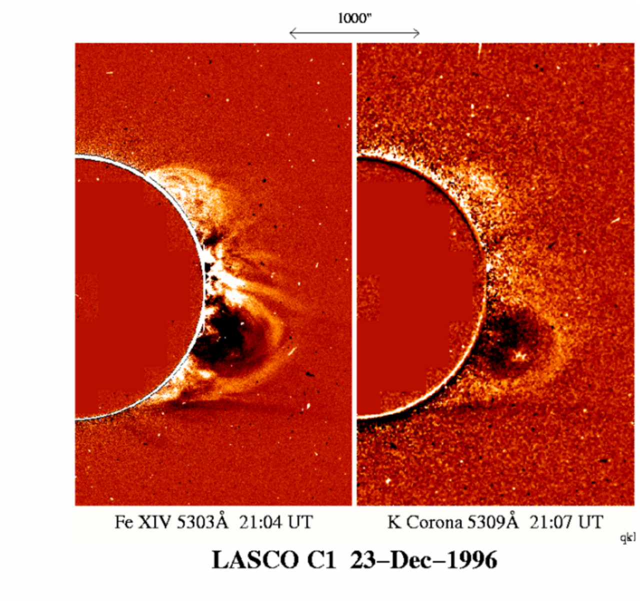

Coronal Mass Ejection (SOHO-LASCO) in forbidden Fe line

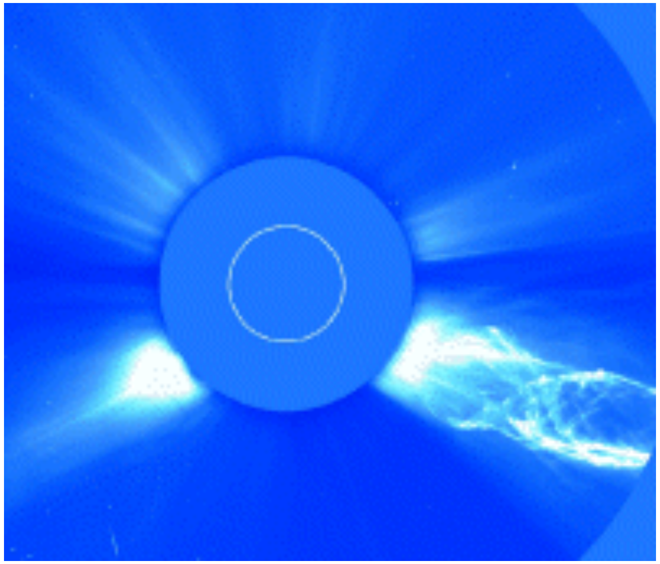

Large CME observed with SOHO coronograph

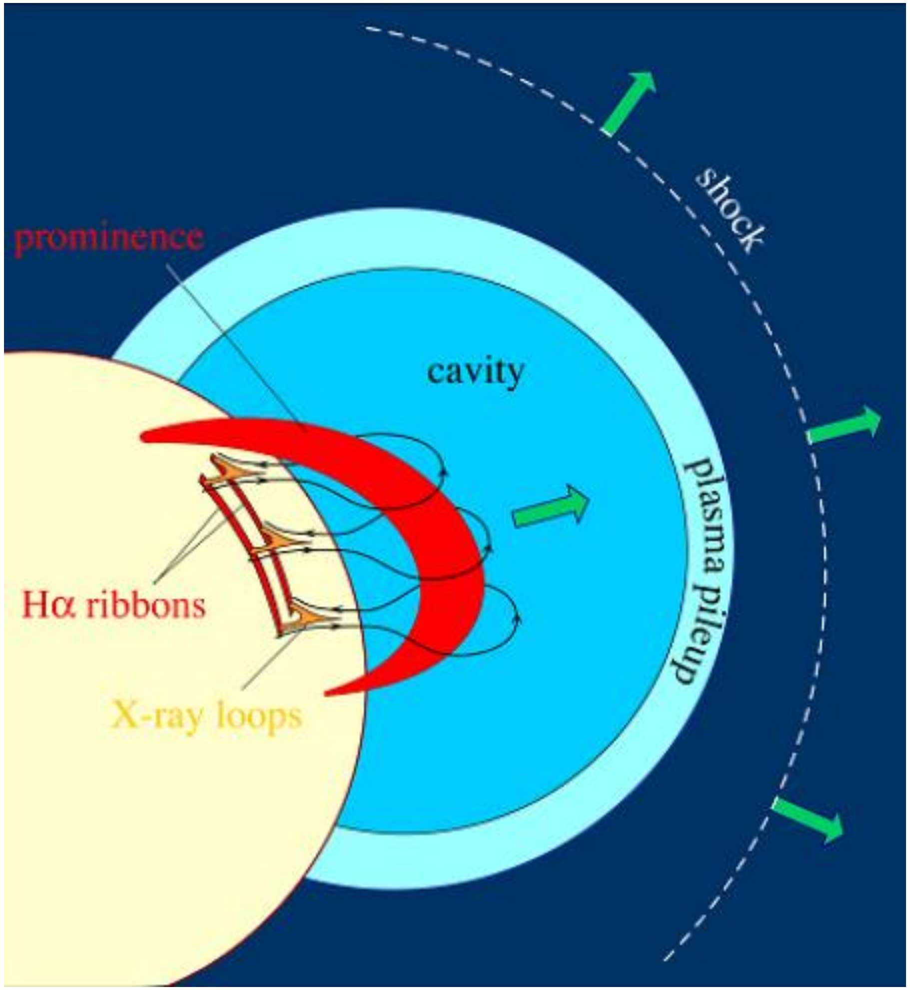
shock
prominence
cavity
plasma pileup
Hα ribbons
X-ray loops

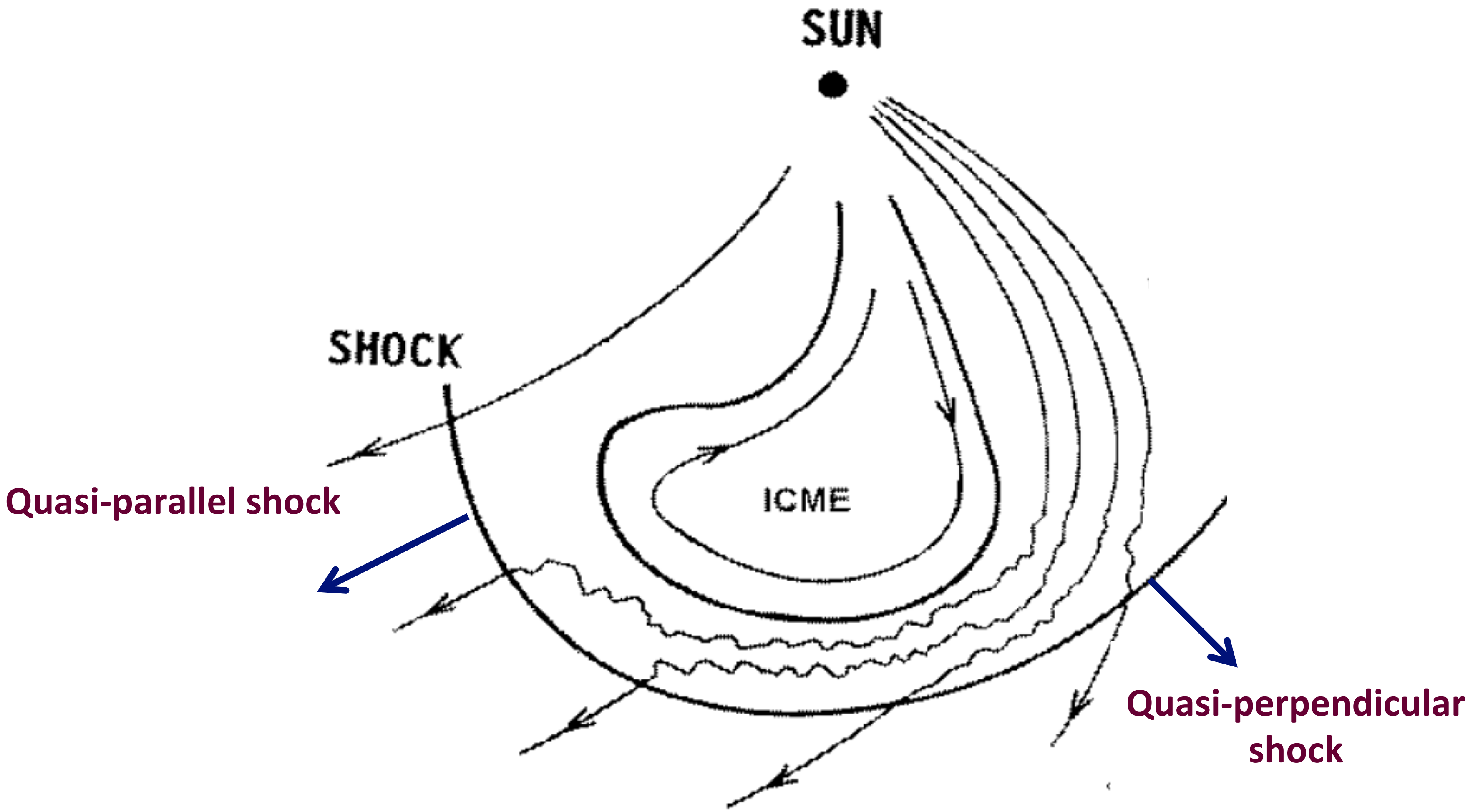
SUN
SHOCK
ICME
Quasi-parallel shock
Quasi-perpendicular shock

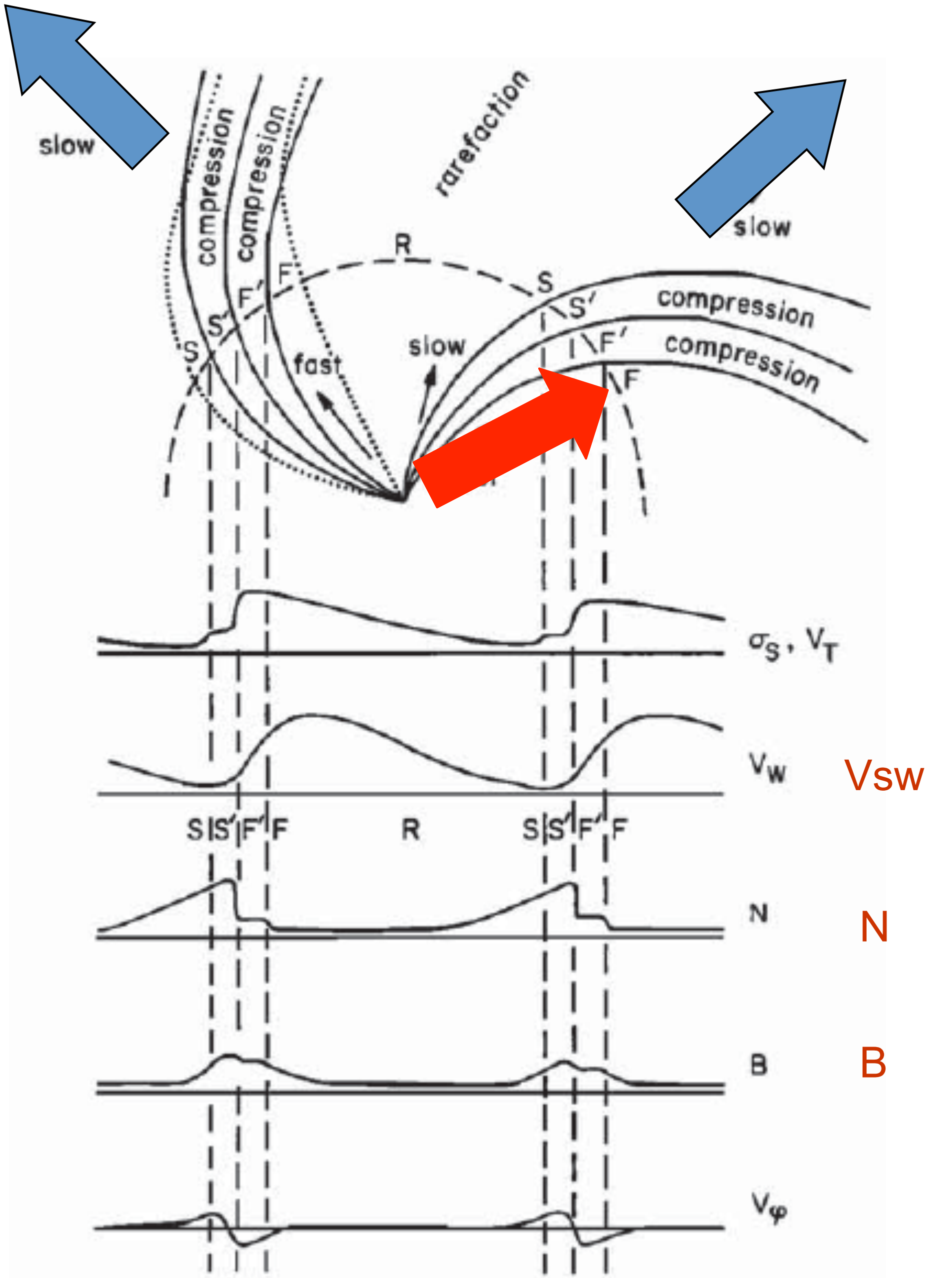

Belcher and Davis 1971

Corotating interaction regions and forward and reverse shock

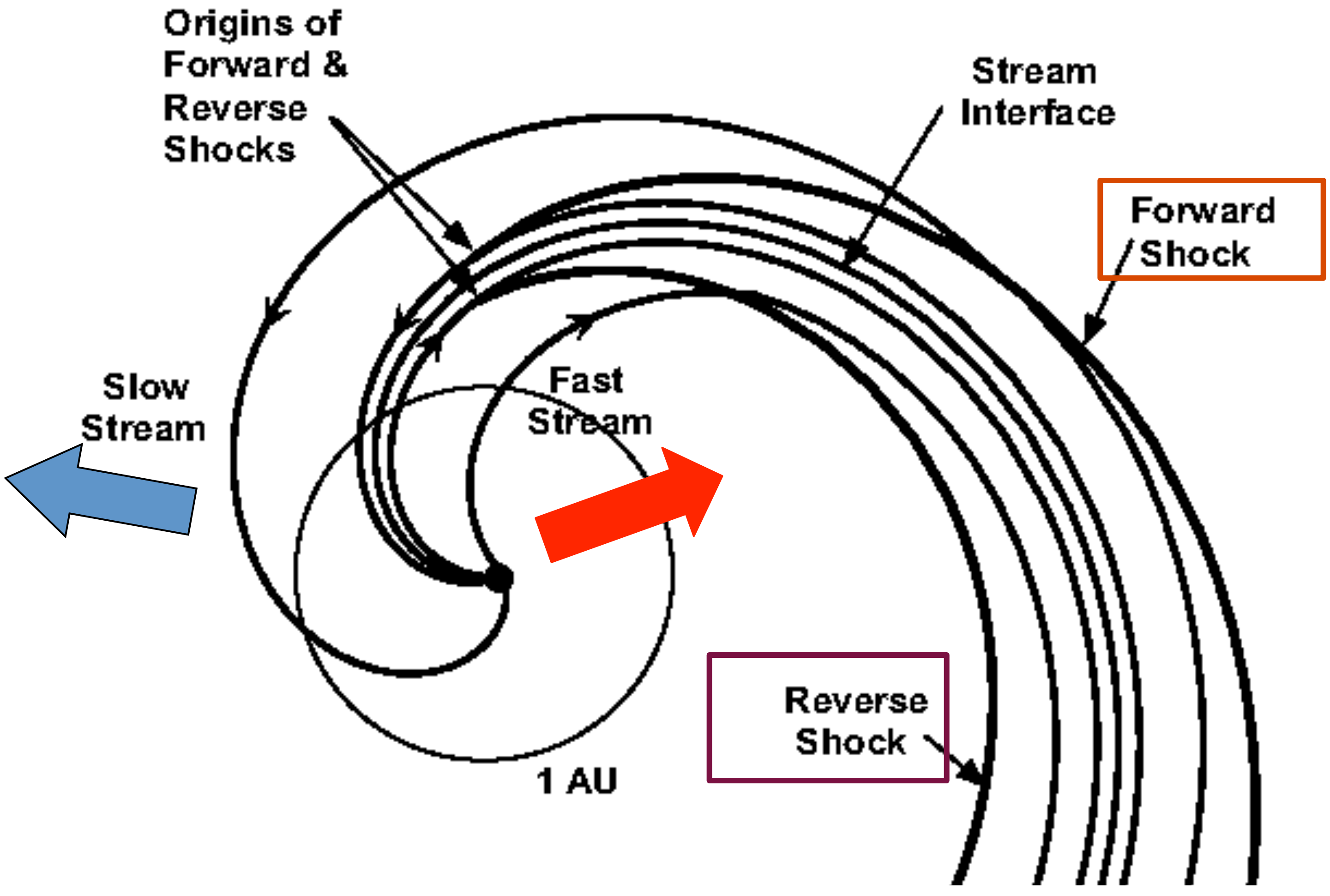

CIR observed by Ulysses at 5 AU

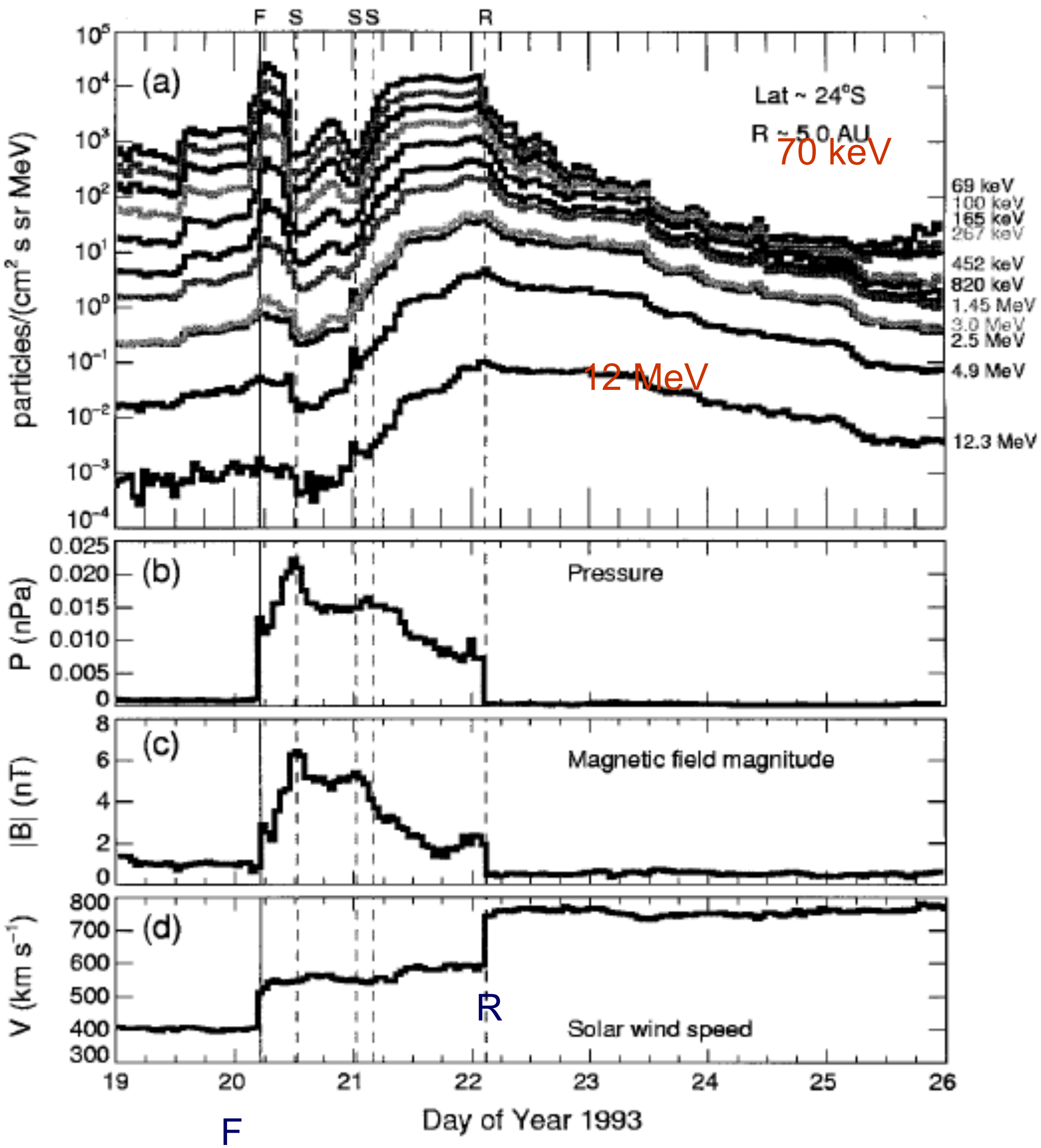

Decker et al. 1999

Earth‘s bow shock

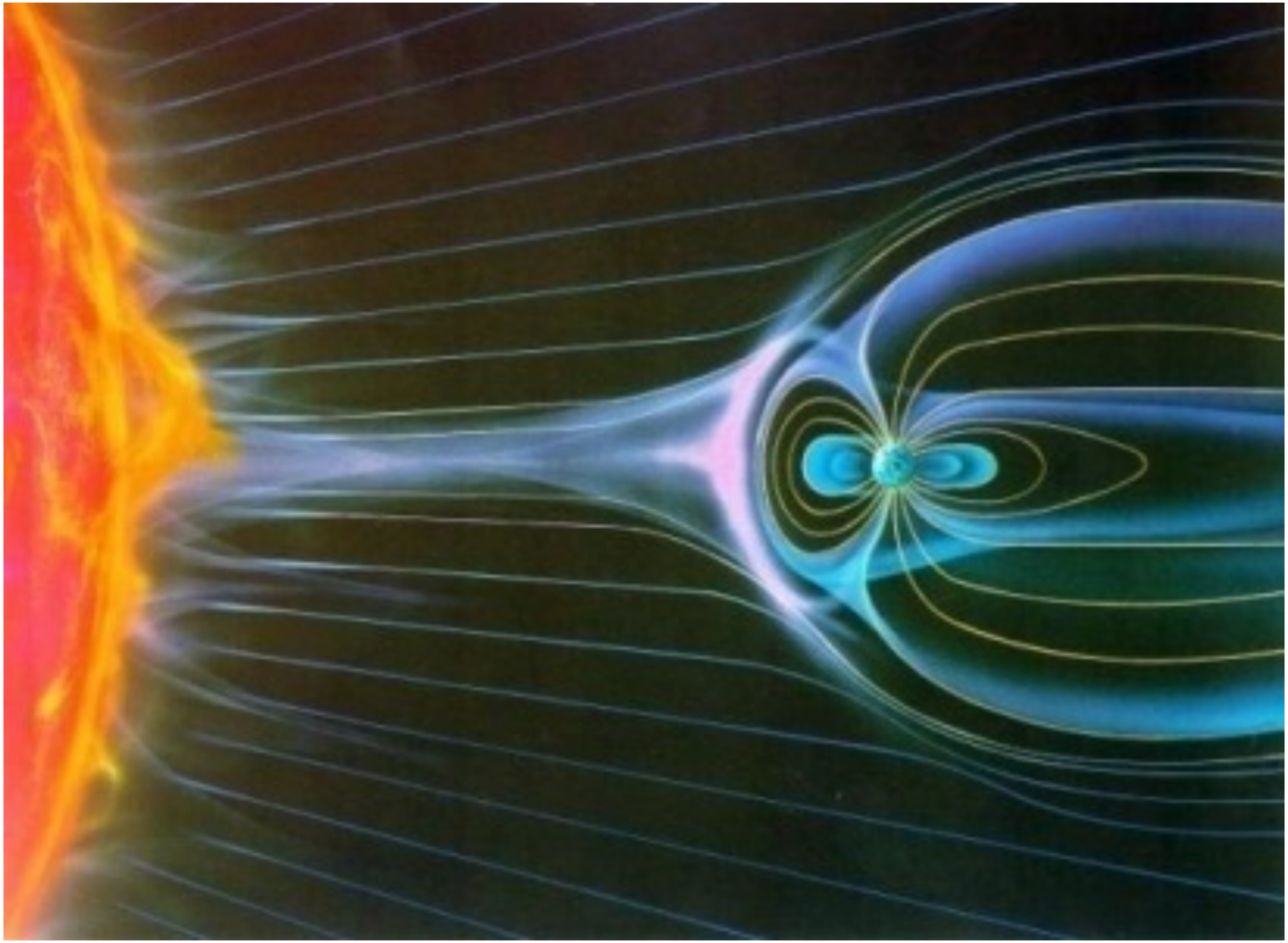

The Earth's Bow Shock

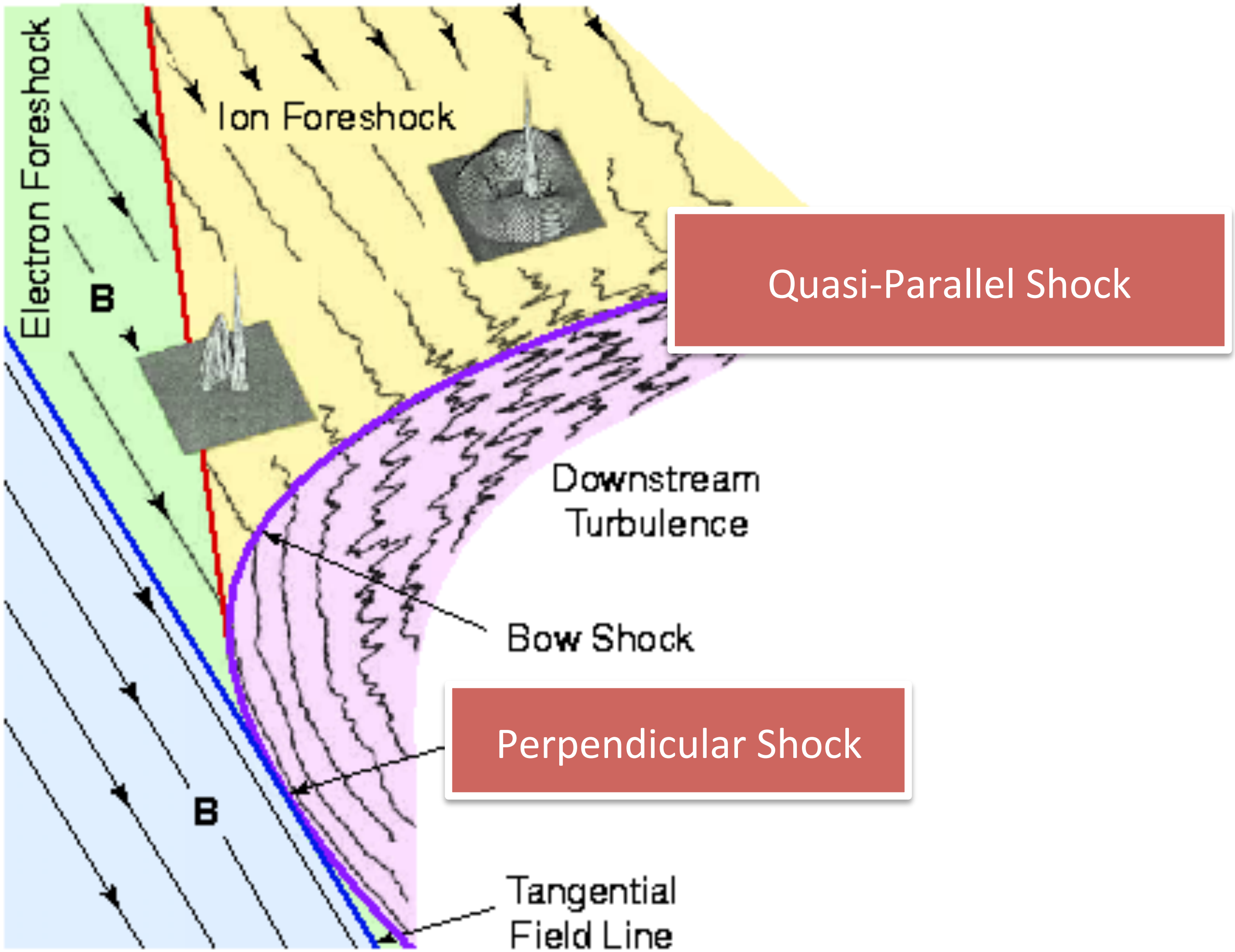

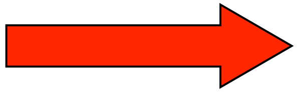

Magnetic field during various bow shock crossings

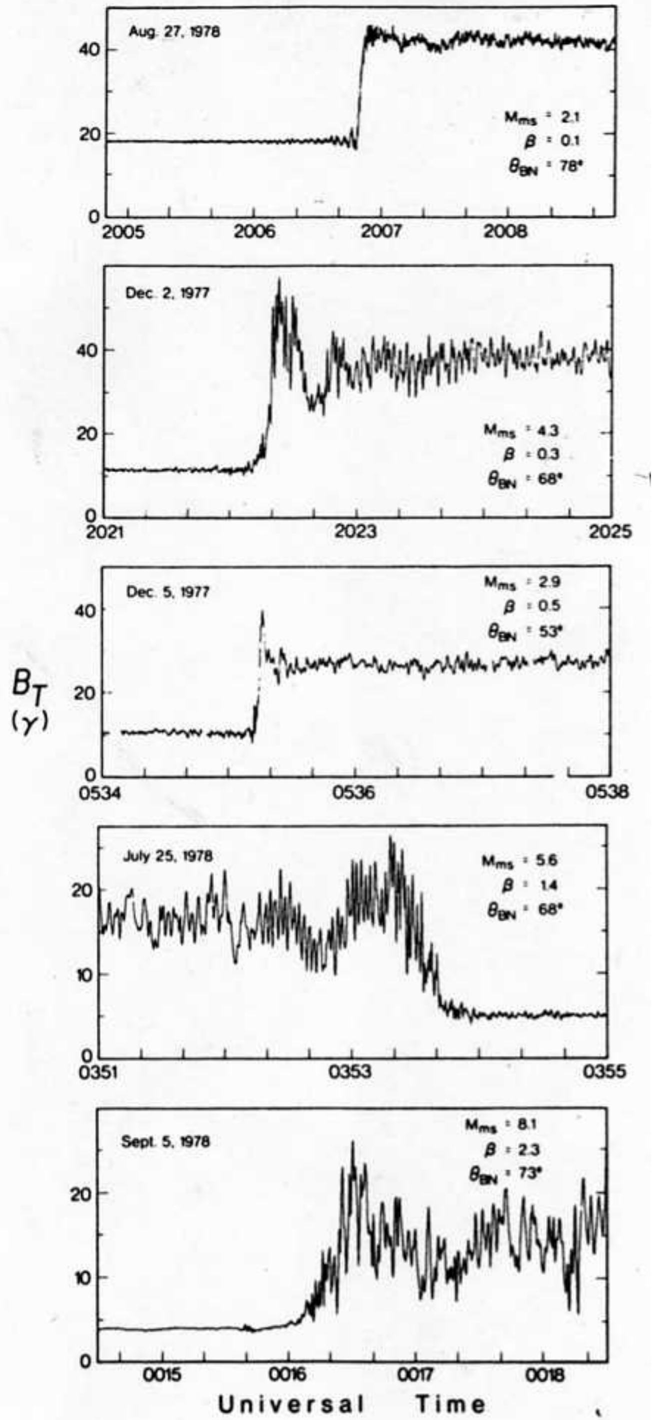

Heliospheric termination shock

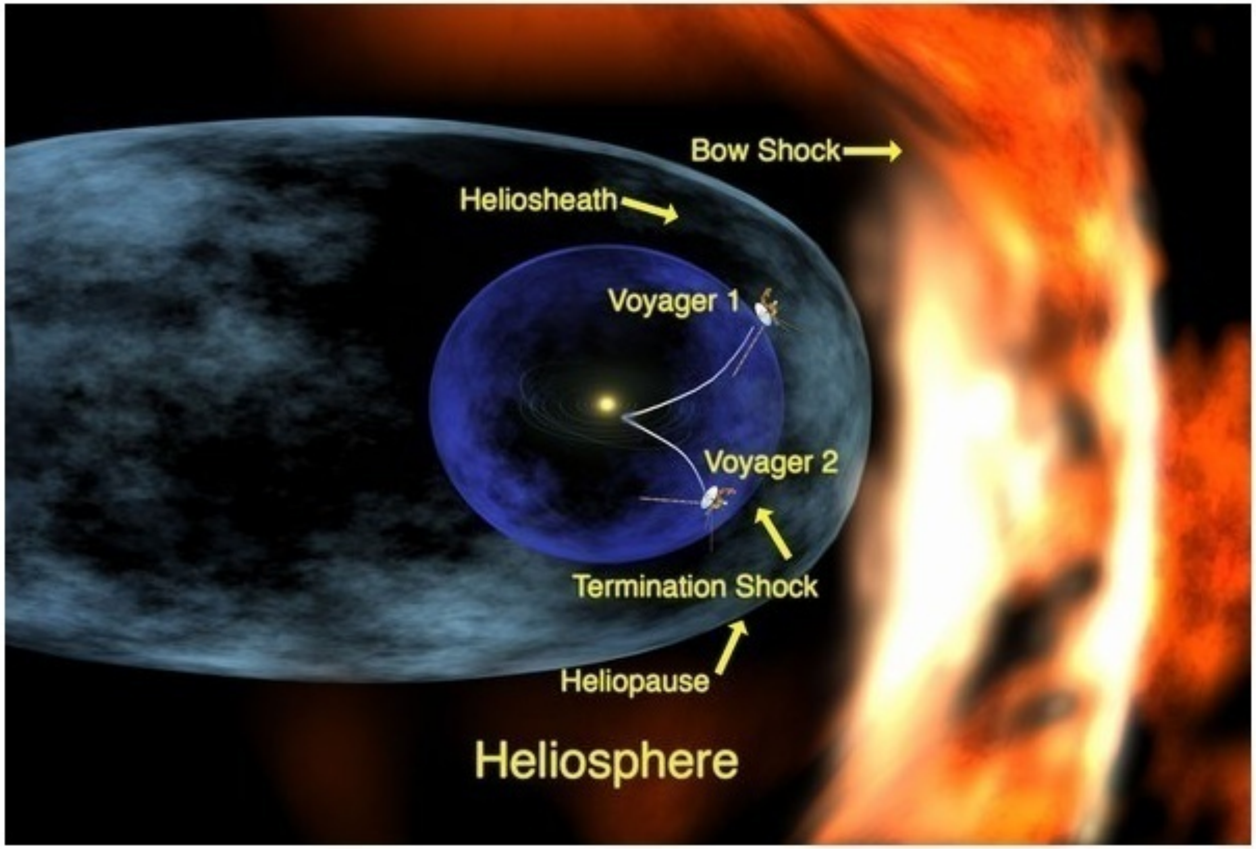

Schematic of the heliosphere showing the heliospheric termination shock (at about 80 – 90 AU) and the bow shock in front of the heliosphere.

Voyager 2 at the termination shock (84 AU)

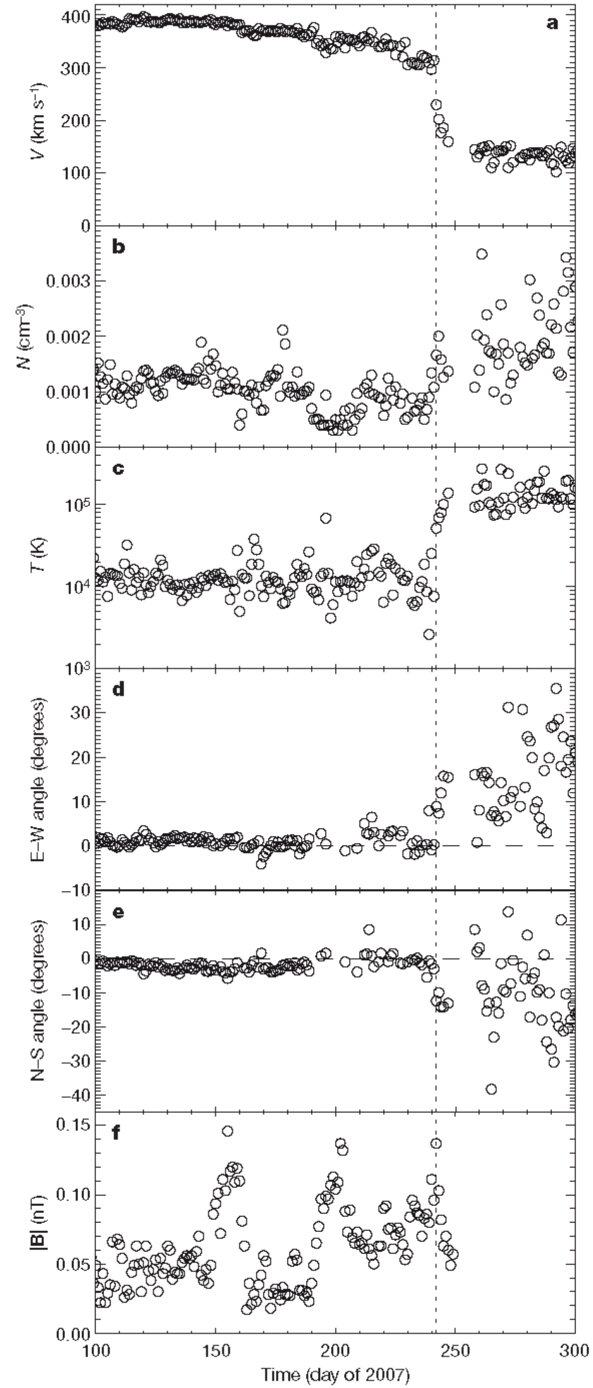

MHD CONSERVATION RELATIONS

MHD Wave Modes

Sound speed in ideal gas

$$c_s = (\gamma \frac{p}{\rho})^{1/2}$$

Alfvén velocity

$$V_A = \frac{B}{(\mu_0 \rho)^{1/2}}$$

Magnetosonic velocity

$$c_{ms}^2 = \frac{1}{2}\{(V_A^2 + c_s^2) \pm [(V_A^2 + c_s^2)^2 - 4 v_A c_s^2 \cos^2\theta]^{1/2}\}$$

Positive root: fast magnetosonic wave mode c_f
Negative root: slow magnetosonic wave mode c_{sl}

Intermediate mode (shear-Alfvén wave):

$$c_{int} = V_A \cos\theta$$

MHD CONSERVATION RELATIONS

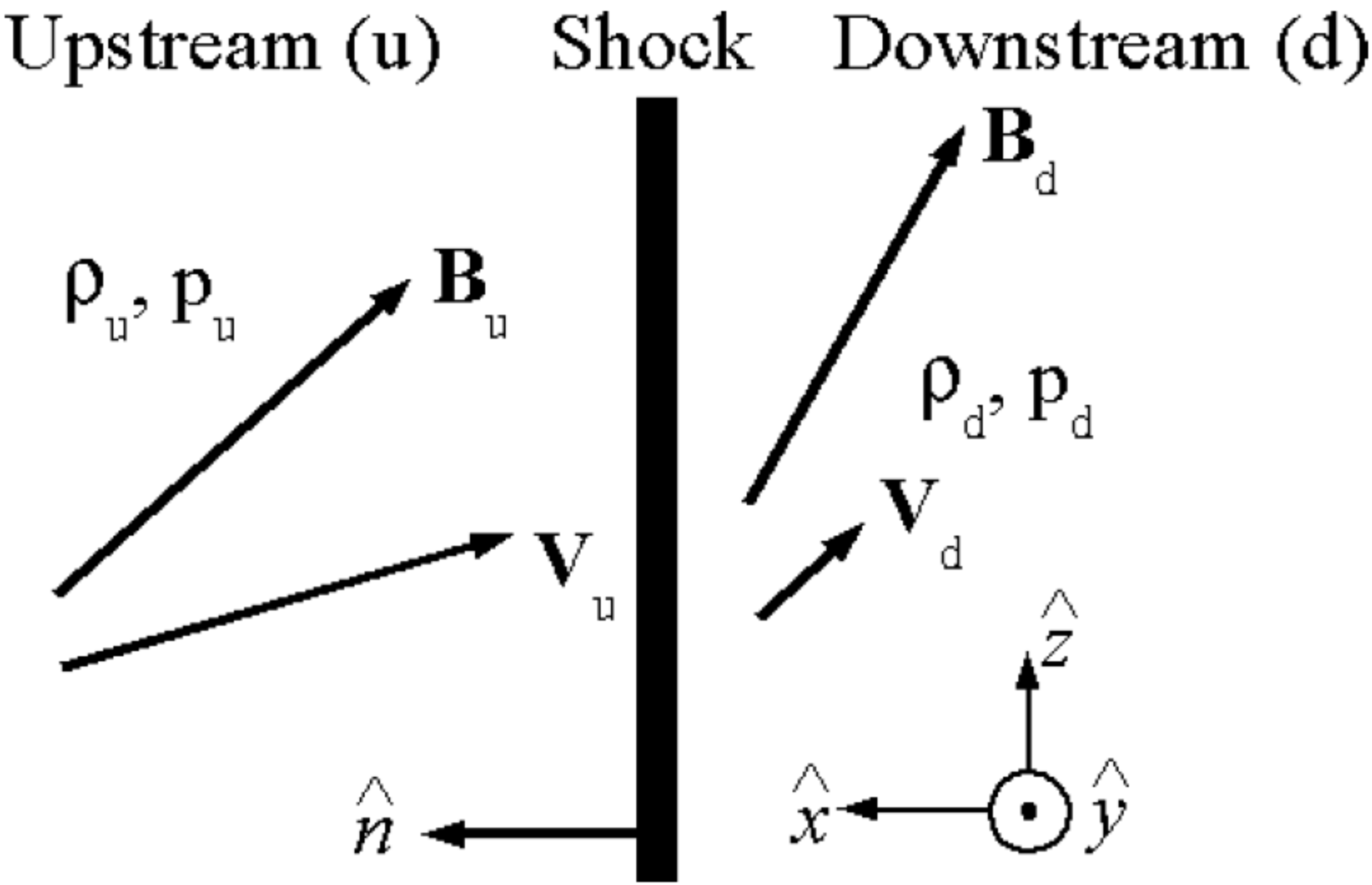

MHD CONSERVATION RELATIONS

$$\frac{\partial Q}{\partial t} + \nabla \cdot \mathbf{F} = 0$$

Conservation equation for a quantity Q with flux F

$$\frac{d}{dx}(F_x) = 0$$

Assume one dimensional and time stationary

[*F*] notation for difference in *F* upstream to downstream

$$[F_n] = 0$$

Integrate upstream to downstream to find that change in flux F normal to shock surface is zero

Conservation of mass

$$\frac{d}{dx}(\rho V_x) = 0 \longrightarrow [\rho V_x] = 0$$

MHD CONSERVATION RELATIONS

$$\left[\rho V_x^2 + p + \frac{B^2}{2\mu_0}\right] = 0$$

$$\left[\rho V_x \mathbf{V}_t - \frac{B_x}{\mu_0}\mathbf{B}_t\right] = 0$$

$$\left[\rho V_x \left(\frac{1}{2}V^2 + \frac{\gamma}{\gamma - 1}\frac{p}{\rho}\right) + V_x \frac{B^2}{\mu_0} - \mathbf{V}\cdot\mathbf{B}\frac{B_n}{\mu_0}\right] = 0$$

$$[B_x] = 0$$

$$[V_x \mathbf{B}_t - B_x \mathbf{V}_t] = 0$$

Discontinuities

Contact Discontinuity	$\mathbf{V}_u = \mathbf{0}$, $B_n \neq 0$	Density jump arbitrary, but pressure and all other quantities are continuous.
Tangential Discontinuity	$V_x = 0$, $B_n = 0$	Plasma pressure and field change maintaining static pressure balance.
Rotational Discontinuity	$V_n = B_n/\sqrt{\mu_0 \rho}$	Form of intermediate shock in isotropic plasma, field and flow change direction but not magnitude.

Shock Waves: $\mathbf{V}_u \neq \mathbf{0}$

Parallel Shock	$B_t = 0$	Magnetic field unchanged by shock.
Perpendicular Shock	$B_n = 0$	Plasma pressure and field strength increases at shock.
Oblique Shocks	$B_t \neq 0$, $B_n \neq 0$	
Fast Shock		Plasma pressure and field strength increase at shock, magnetic field bends away from normal.
Slow Shock		Plasma pressure increases, magnetic field strength decreases, magnetic field bends towards normal.
Intermediate Shock		Only shocklike in anisotropic plasma.

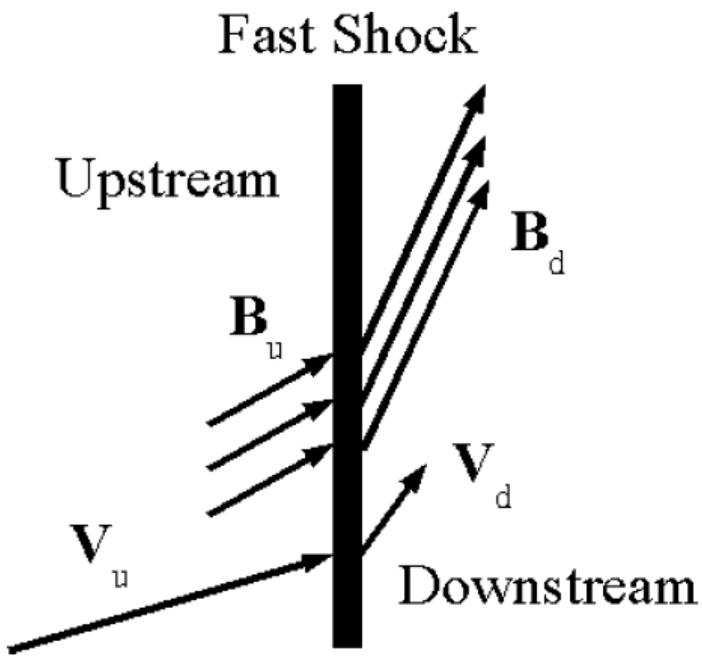

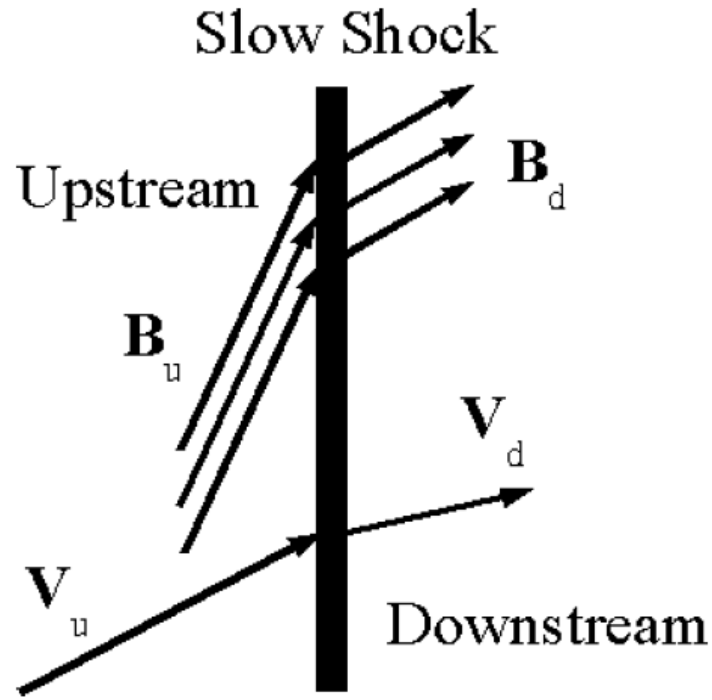

$V_{n,u} > V_{f,u}$ and $V_{f,d} > V_{n,d} > V_{A,d}$

$V_{A,u} > V_{n,u} > V_{s,u}$ and $V_{s,d} > V_{n,d}$

SHOCK PARAMETERS

Shock normal angle

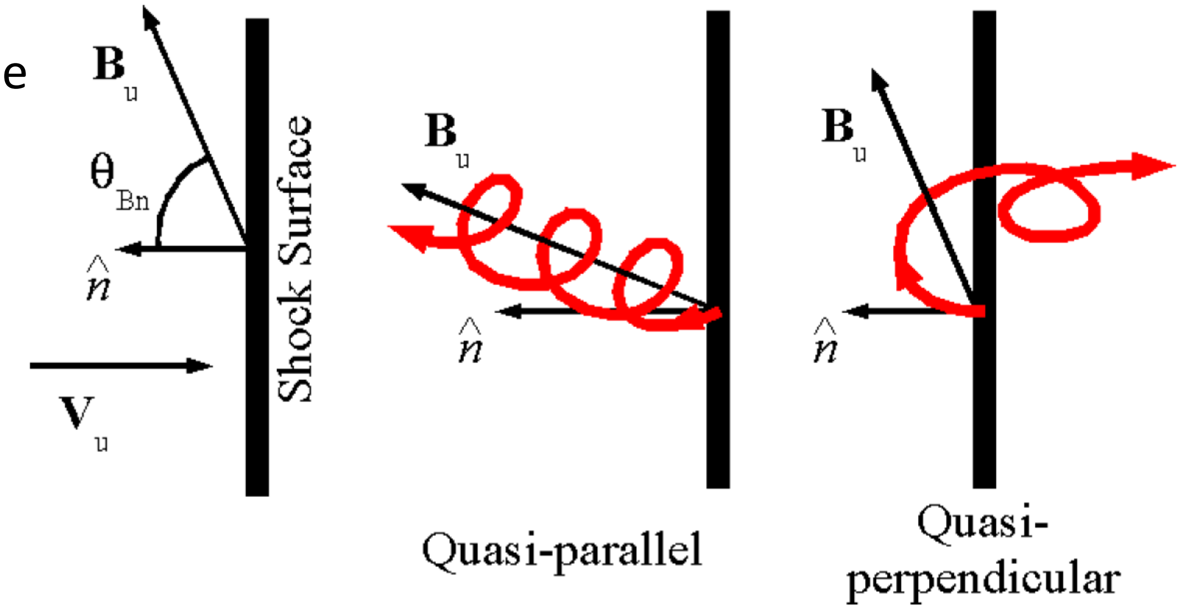

Alfvén Mach Number

$$M_A = \frac{V_u}{B_u / \sqrt{\mu_0 \rho_u}}$$

Other plasma parameters: plasma beta, composition, anisotropy, etc!

USING THE SHOCK CONSERVATION RELATIONS

Exactly parallel shock

$$\mathbf{B}_u = B_x \hat{n},\ \mathbf{B}_{ut} = \mathbf{0}$$

Using transverse momentum equation

$$\left[\left(1 - \frac{B_n^2}{\mu_0 \rho V_n^2} \right) V_n \mathbf{B}_t \right] = \mathbf{0}$$

Transverse magnetic field zero upstream and downstream, so magnetic field is unchanged by shock.

Shock jump relations same as for an ordinary gas shock.

USING THE SHOCK CONSERVATION RELATIONS

Exactly perpendicular shock $B_x = 0$ and $\mathbf{B}_u = \mathbf{B}_{ut}$

From conservation of tangential electric field $V_{ux}\mathbf{B}_{ut} = V_{dx}\mathbf{B}_{dt}$

density *compression ratio* $r = \rho_d / \rho_u$

Magnetic field compresses as much as the density

For high Mach number, compression ratio becomes

$$r = \frac{\gamma + 1}{\gamma - 1}$$

$M_A \gg 1$ and $M_{cs} \gg 1$

Compression ratio has limit of about 4 as Mach number increases

de Hoffmann-Teller Frame (H-T frame) and Normal Incidence Frame (NIF frame)

θ_{Bn} = angle between $\vec{B}$ and $\vec{n}$

θ_{Vn} = angle between $\vec{V}$ and $\vec{n}$

If $\theta_{Vn} = 0$: Normal Incidence Frame (NIF)

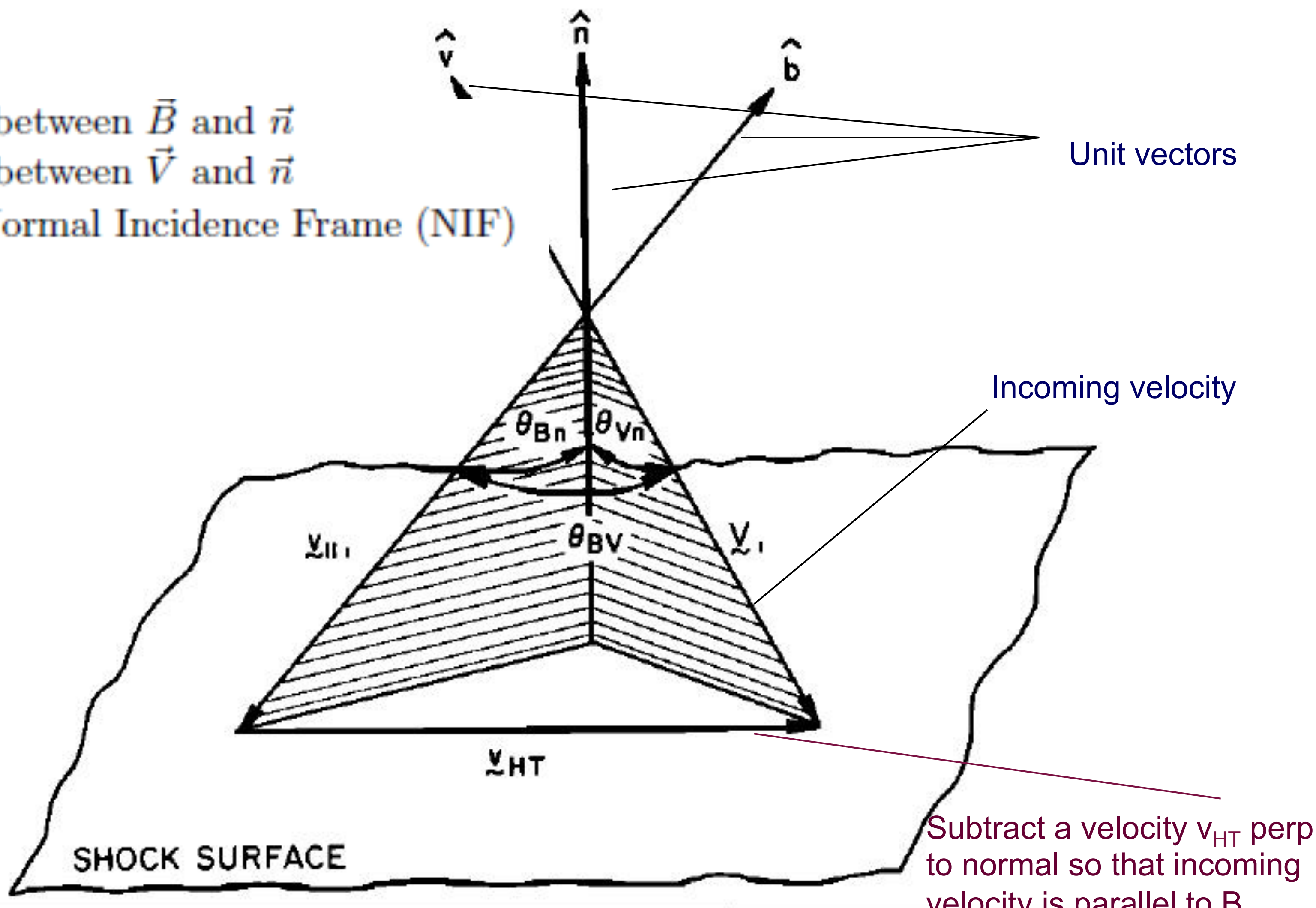

The de Hoffmann-Teller velocity

$\vec{V}_{in}$ = incoming velocity, $\vec{V}_{HT}$ = de Hoffmann-Teller velocity, $\vec{V}^*_{in}$ = incoming velocity in the H-T frame

$$\vec{V}_{in} = \vec{V}_{HT} + \vec{V}^*_{in}$$

Take cross-product with $\vec{B}$

$$\vec{B} \times \vec{V}^*_{in} = 0 = \vec{B} \times \vec{V}_{in} - \vec{B} \times \vec{V}_{HT}$$

take cross-product with $\vec{n}$

$$\vec{n} \times (\vec{B} \times \vec{V}_{HT}) = \vec{n} \times (\vec{B} \times \vec{V}_{in})$$

$$\vec{n} \times (\vec{B} \times \vec{V}_{HT}) = \vec{B}(\vec{n} \cdot \vec{V}_{HT}) - \vec{V}_{HT}(\vec{n} \cdot \vec{B})$$

$$\vec{V}_{HT} = -\frac{\vec{n} \times (\vec{B} \times \vec{V}_{in})}{\vec{n} \cdot \vec{B}}$$

1. Since in the de Hoffmann -Teller (HT) frame the velocity is parallel to the magnetic field the $\vec{V} \times \vec{B}$ electric field vanishes in that frame

2. In the HT frame the shock is at rest - no induced electric field

A consequence of $\vec{E} = 0$ is that the energy of a particle is constant, and surfaces of constant particle energy are spheres centered on the HT frame origin

3. The de Hoffmann-Teller transformation velocity is the same downstream as it is upstream

de HOFFMAN-TELLER FRAME

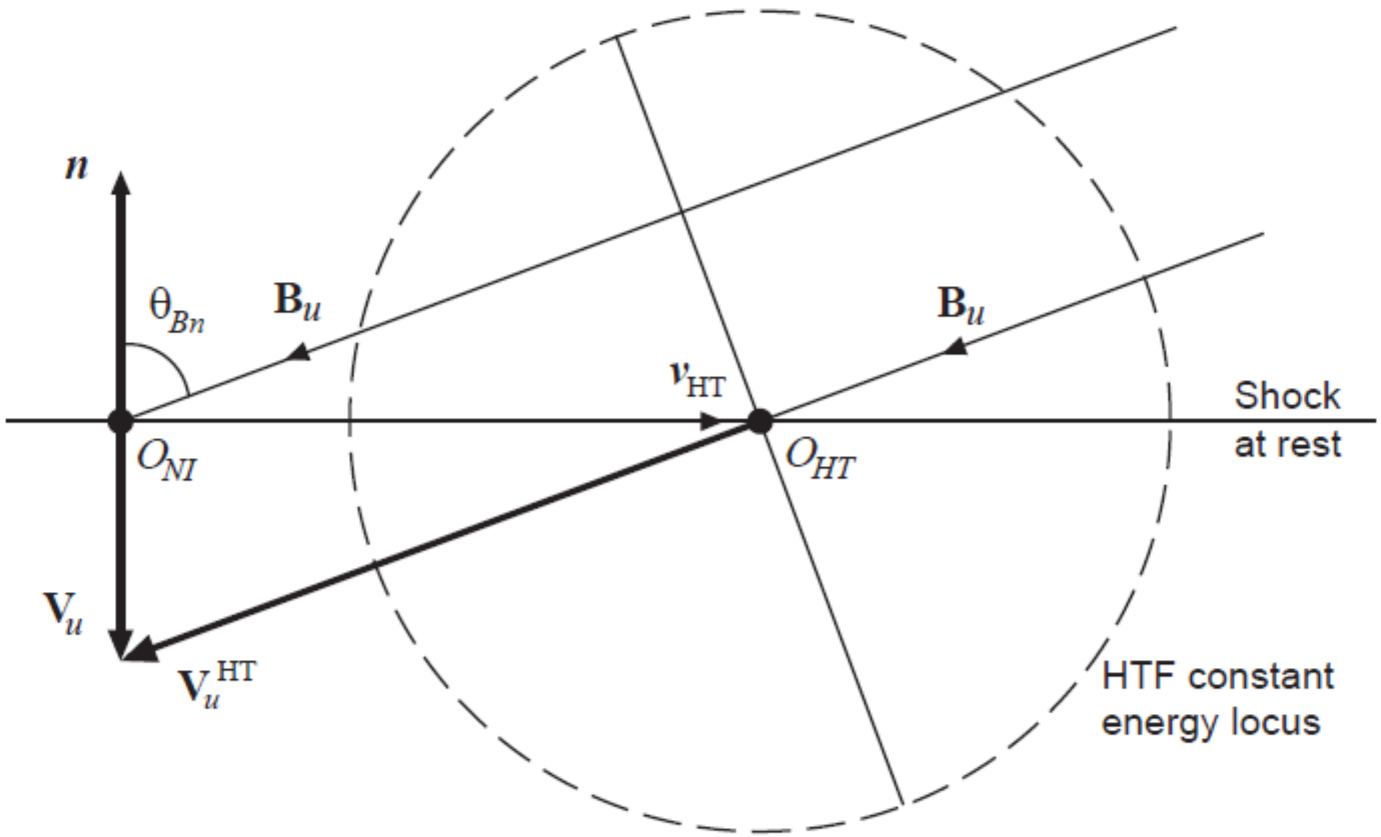

$$v_{\mathrm{HT}} = V_u \tan\theta_{Bn}$$

SHOCKS IN COLLISIONLESS PLASMA

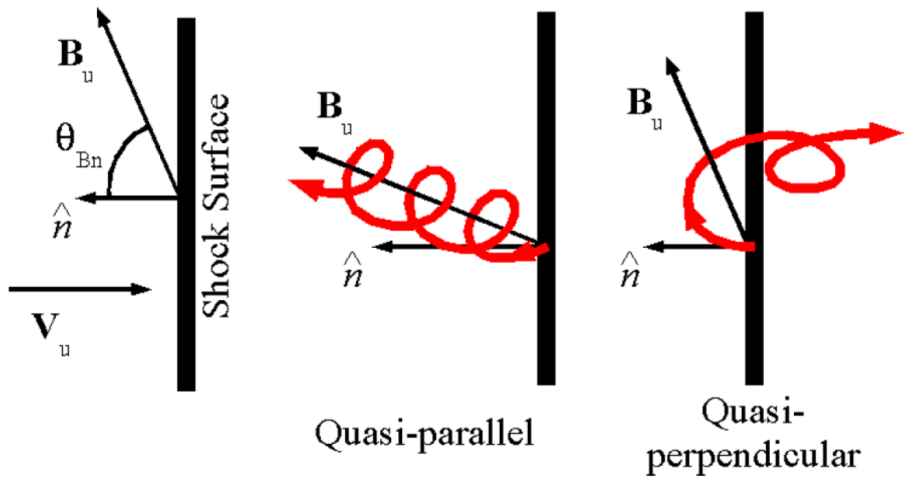

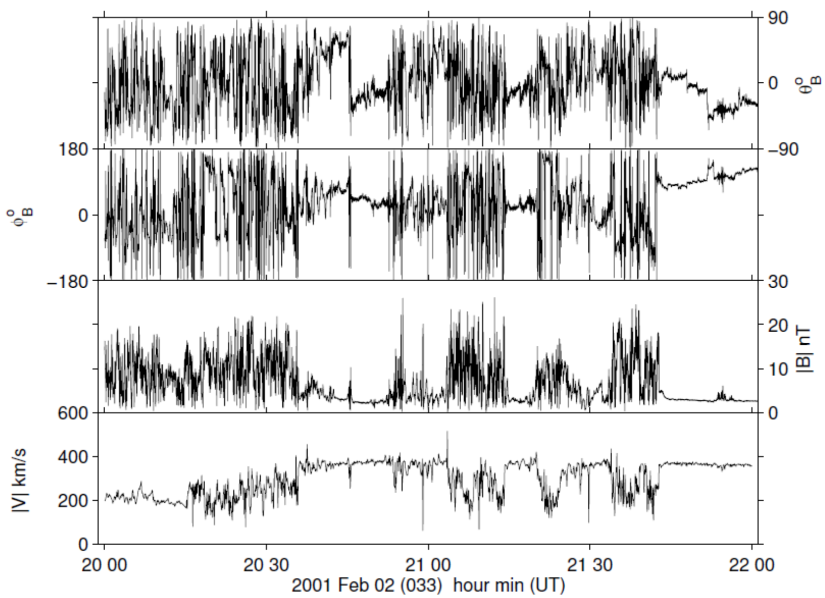

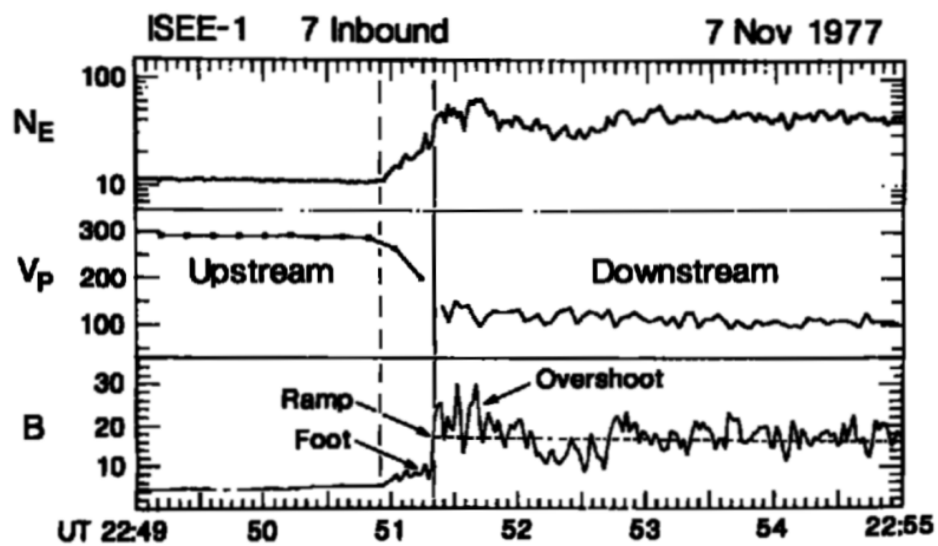

ION REFLECTION AND SHOCK STRUCTURE

QUASI-PERPENDICULAR

Ion reflection leads to a heated downstream distribution

Sun ←

Solar wind

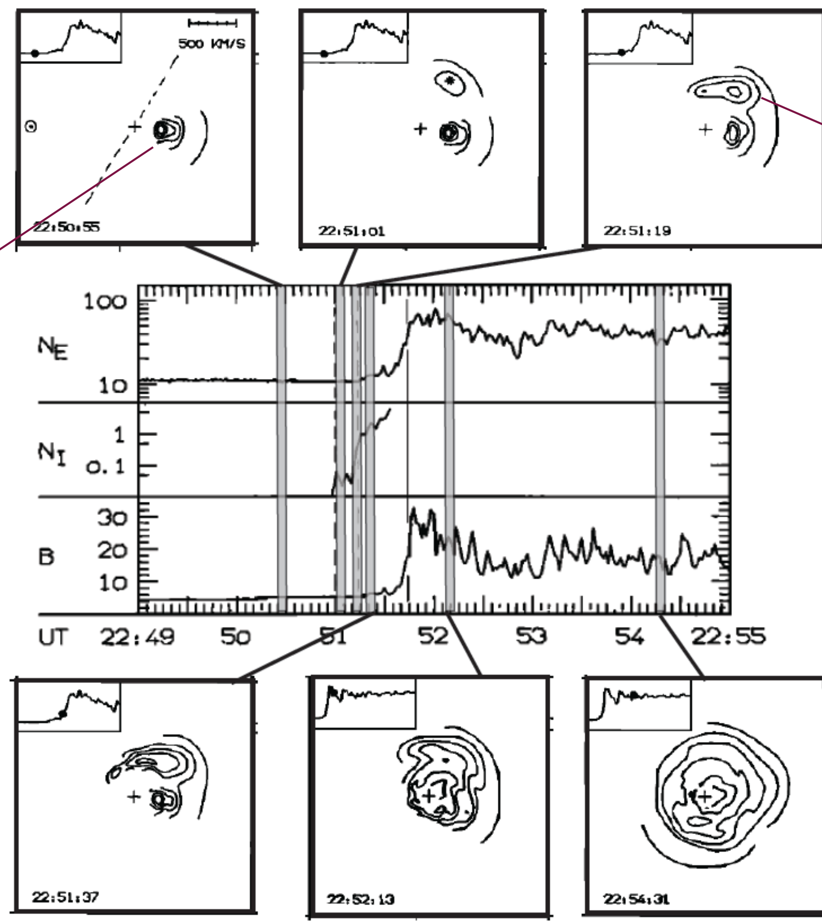

Specularly reflected ions

ION REFLECTION AND SHOCK STRUCTURE

QUASI-PERPENDICULAR

Ion reflection leads to a heated downstream distribution

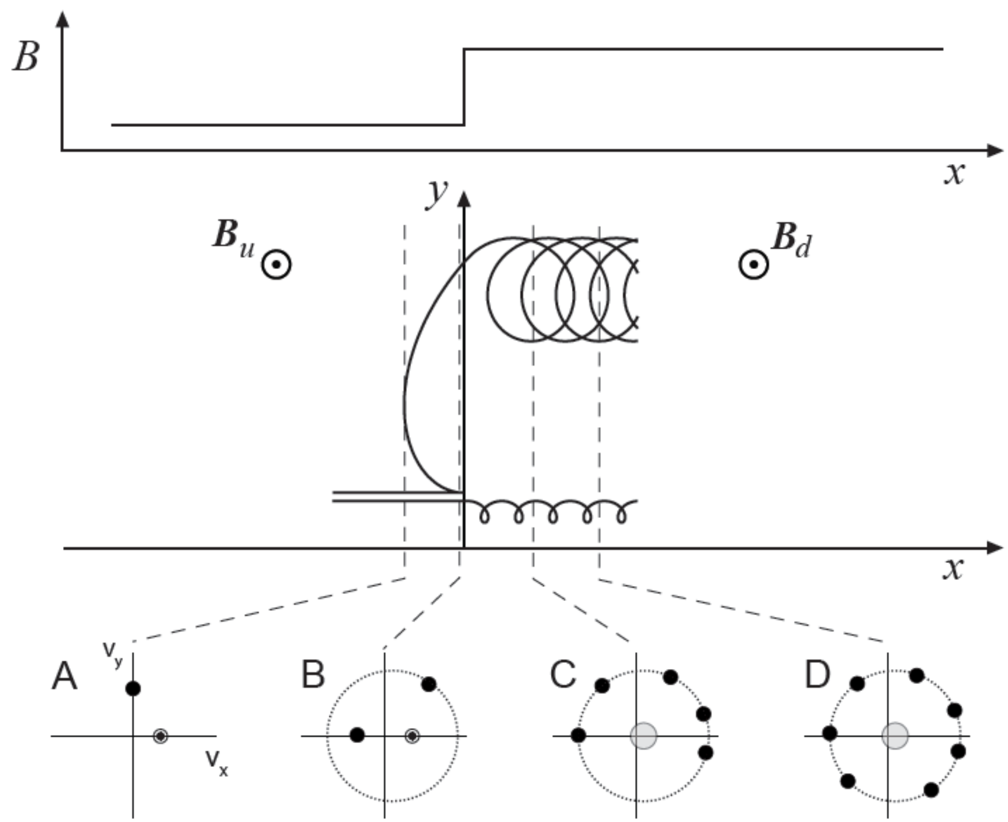

Velocity space

ION REFLECTION AND SHOCK STRUCTURE

QUASI-PARALLEL

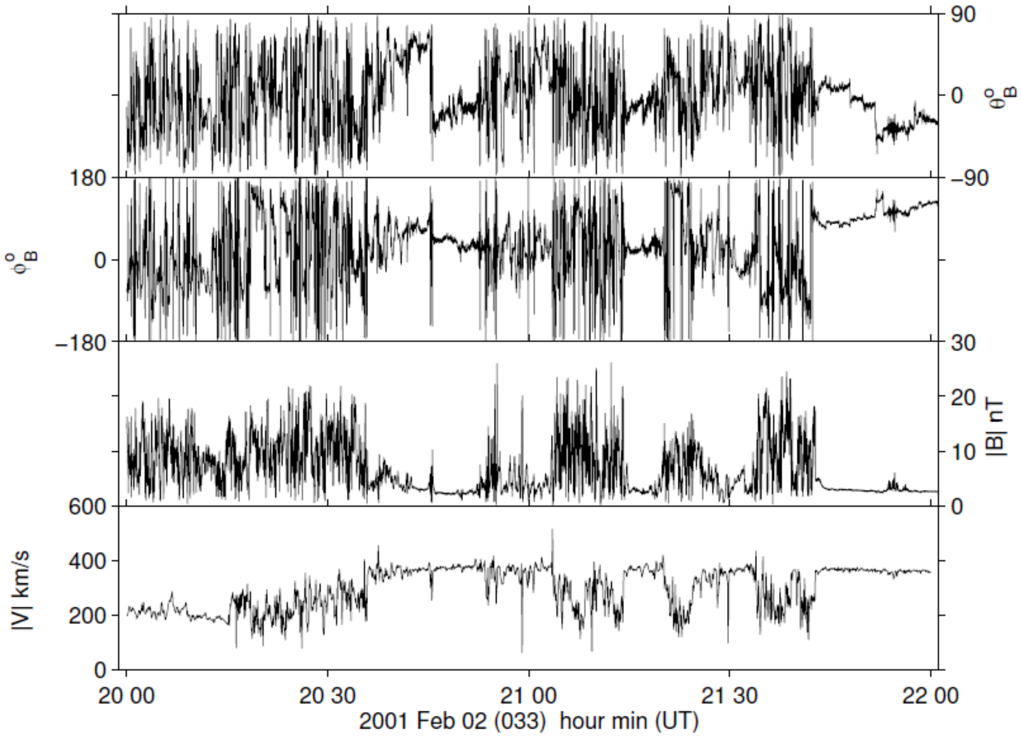

Ion reflection leads to upstream energetic particles and upstream (and downstream) turbulence

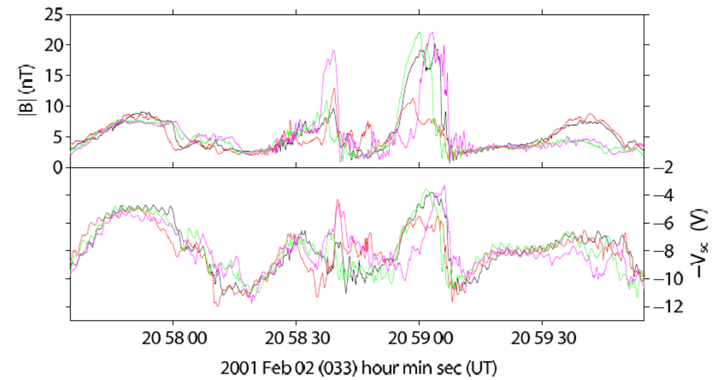

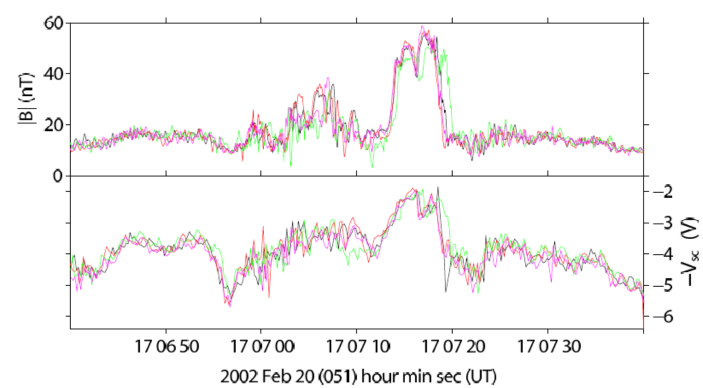

Large amplitude magnetic pulsations

SIMULATION OF PARALLEL AND QUASI-PERPENDICULAR SHOCKS

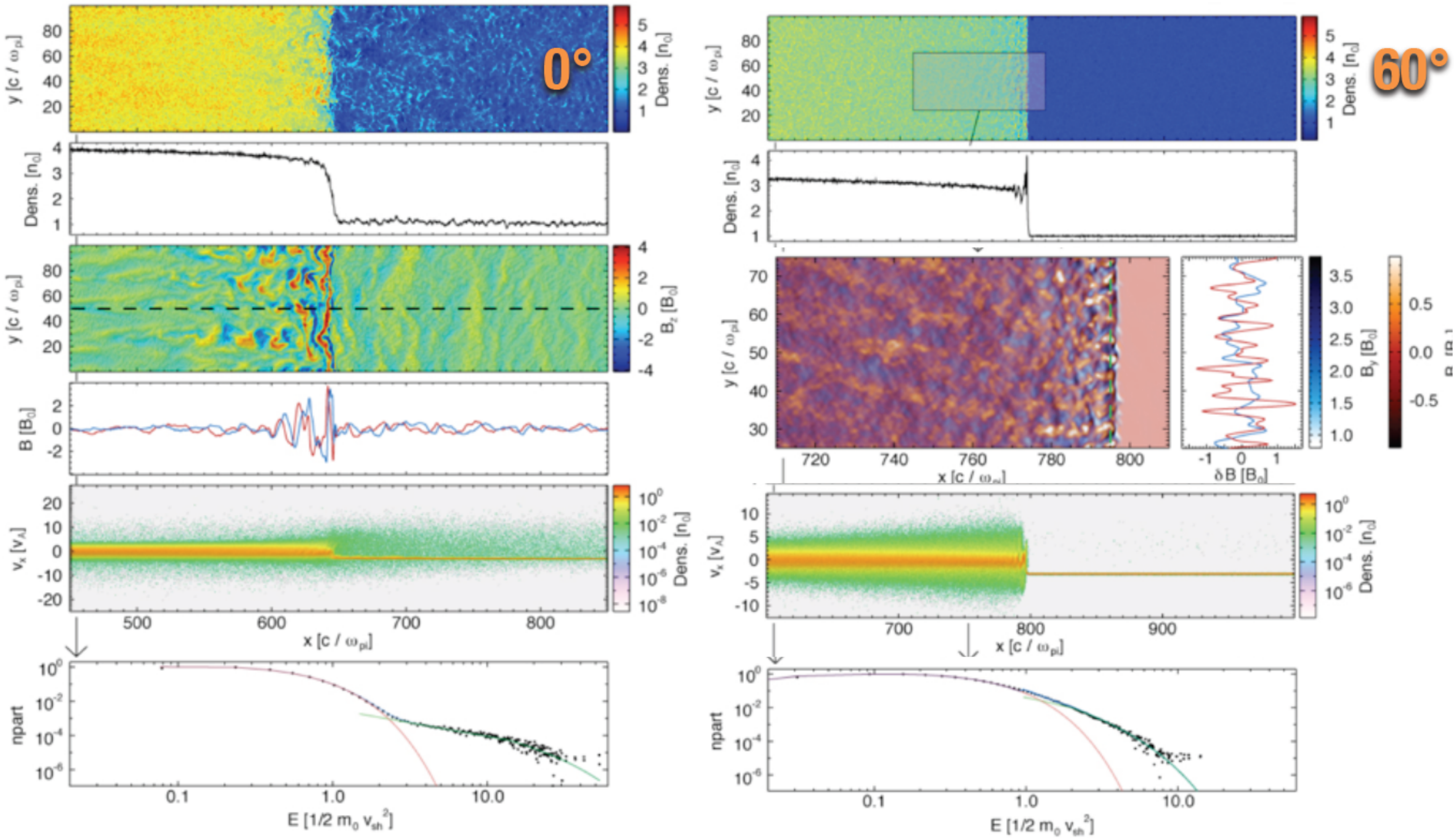

Spitkovksy, 2011

PARTICLE ACCELERATION AT SHOCKS

In a collisionless plasma

- *a small number of particles can reach large energy*

Energetic Particles at Earth's Bow Shock

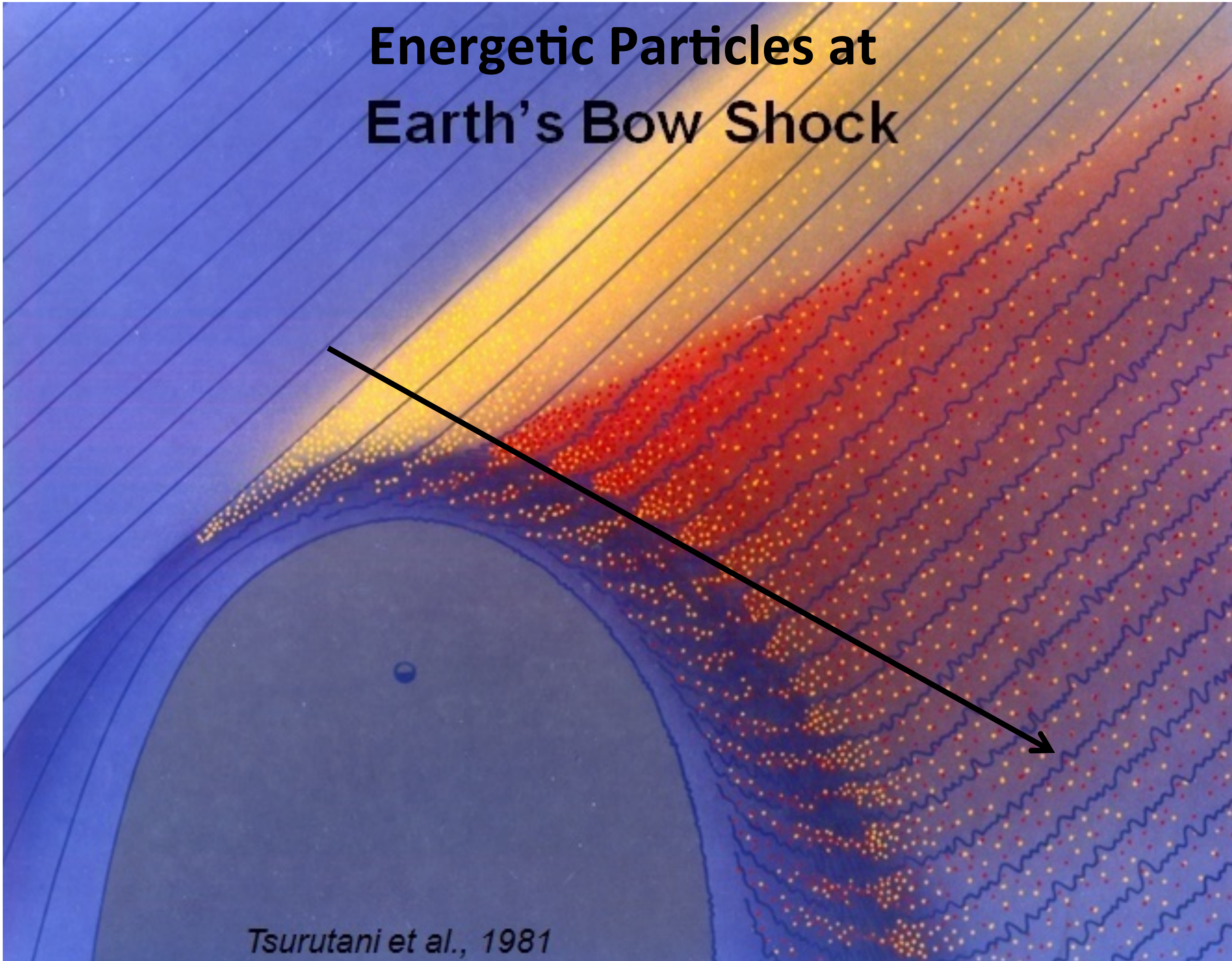

Electron Acceleration at the Quasi-Perpendicular Bow Shock

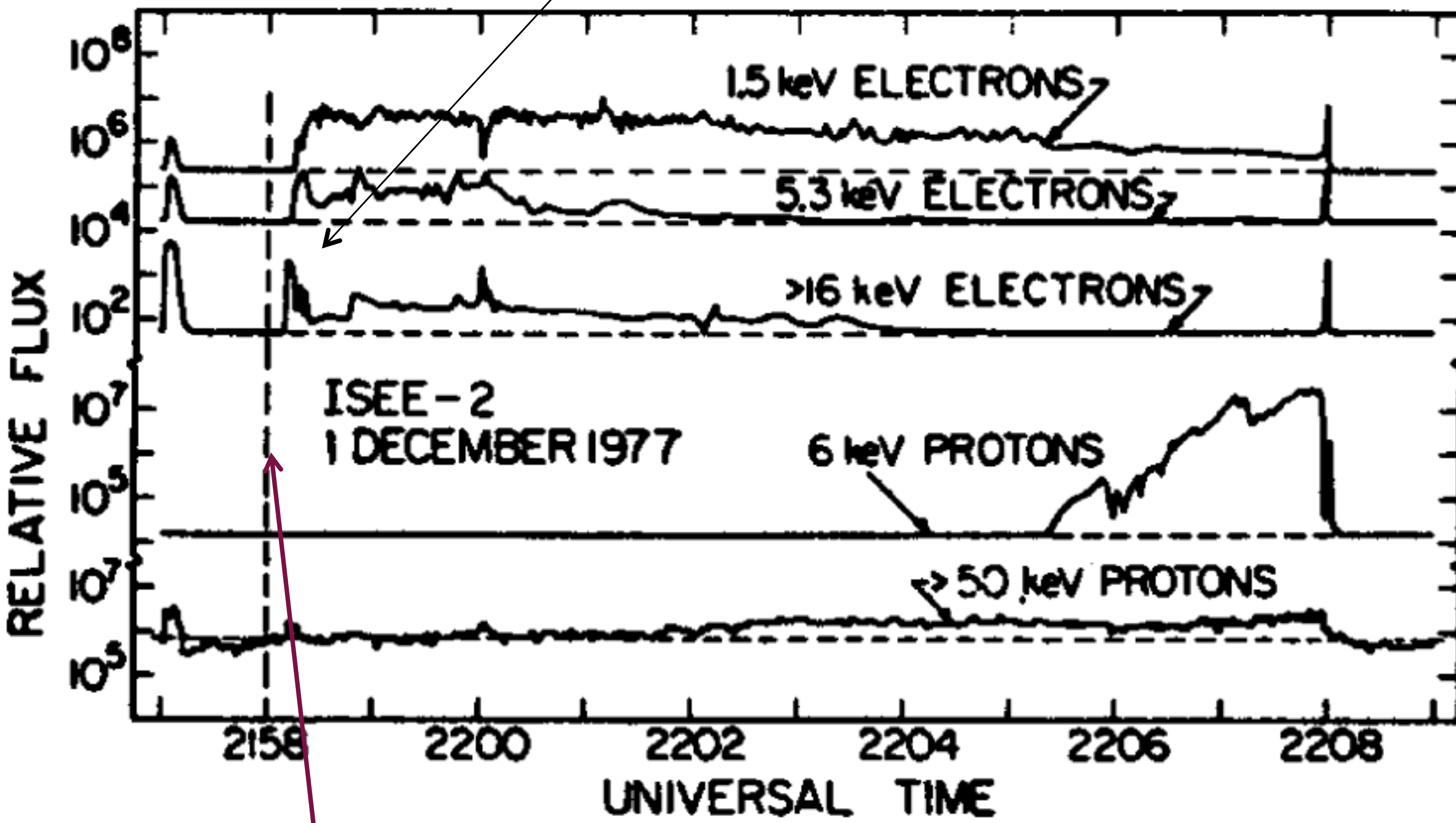

Upstream edge of the foreshock

Anderson et al. 1979

Foreshock velocity dispersion

Most energetic electrons at foreshock edge

Lower energies deeper in the foreshock

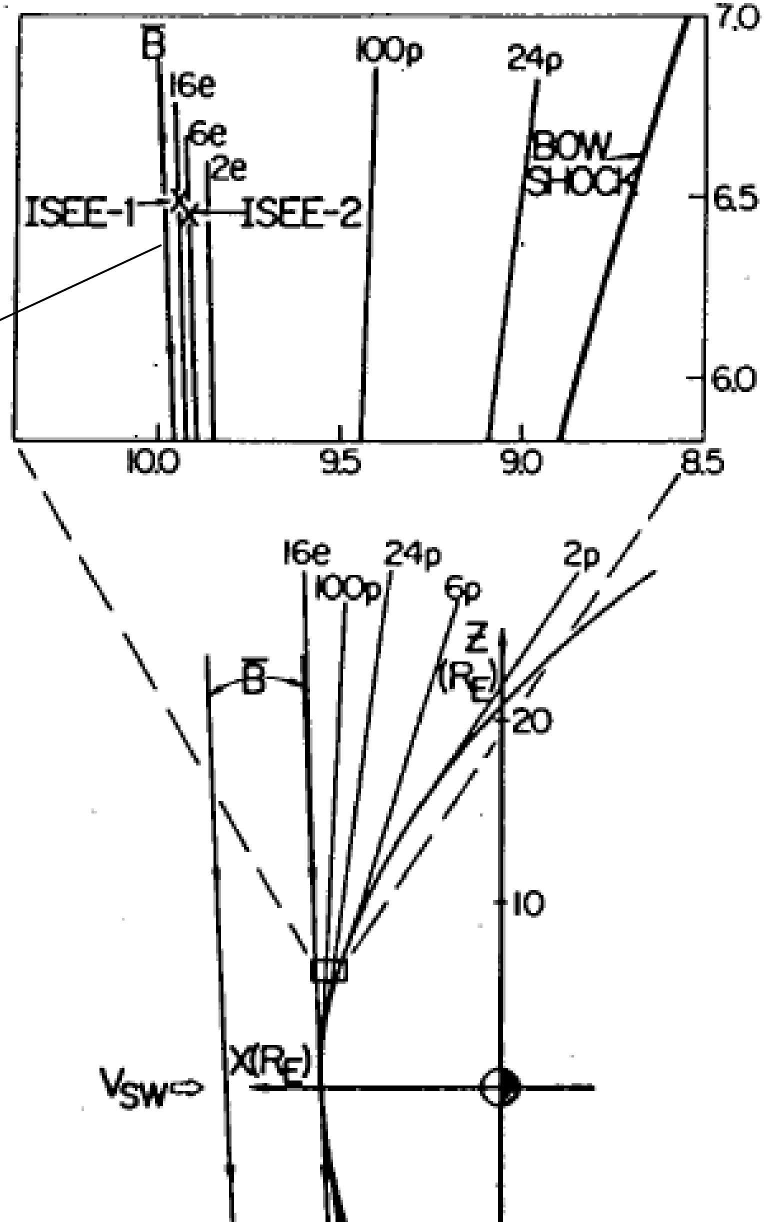

Electron acceleration at the foreshock edge
(quasi-perpendicular shock)

Adiabatic motion of electrons in HT frame:

$$\mu = \frac{m(v^{HT})^2}{2B} = \text{const.}$$

Liouville's theorem: phase space density at point in velocity space is same as incident distribution at point whence reflected particles originated

$$f_r(-v_{\|}^{HT}, v_{\perp}^{HT}) = f_0(v_{\|}^{HT}, v_{\perp}^{HT})$$

But: there is normal electric field (not removed by transformation in HT frame).

Thus energy equation

$$\frac{1}{2}m[v_{\parallel}^{HT}(x_i)]^2 = \frac{1}{2}m[v_{\parallel}^{HT}(x)]^2 + \Psi(x)$$

x_i=initial position upstream and Ψ pseudo-potential ($\phi^{HT}(x)$ electrostatic potential in the HTF)

$$\Psi(x) = \mu[B(x) - B(x_i)] - e\phi^{HT}(x)$$

Effect of potential: lower energy particles that would have been reflected, pass downstream

Reflected electrons: Ring beam with sharp edges

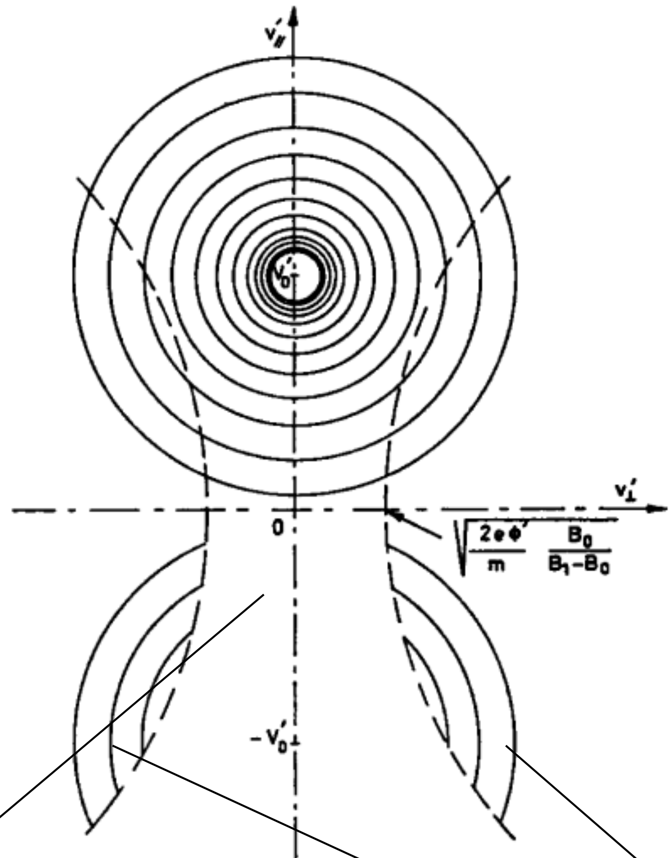

Larger loss cone due to cross-shock potential

Portion reflected by magnetic mirroring modified by effect of cross-shock potential

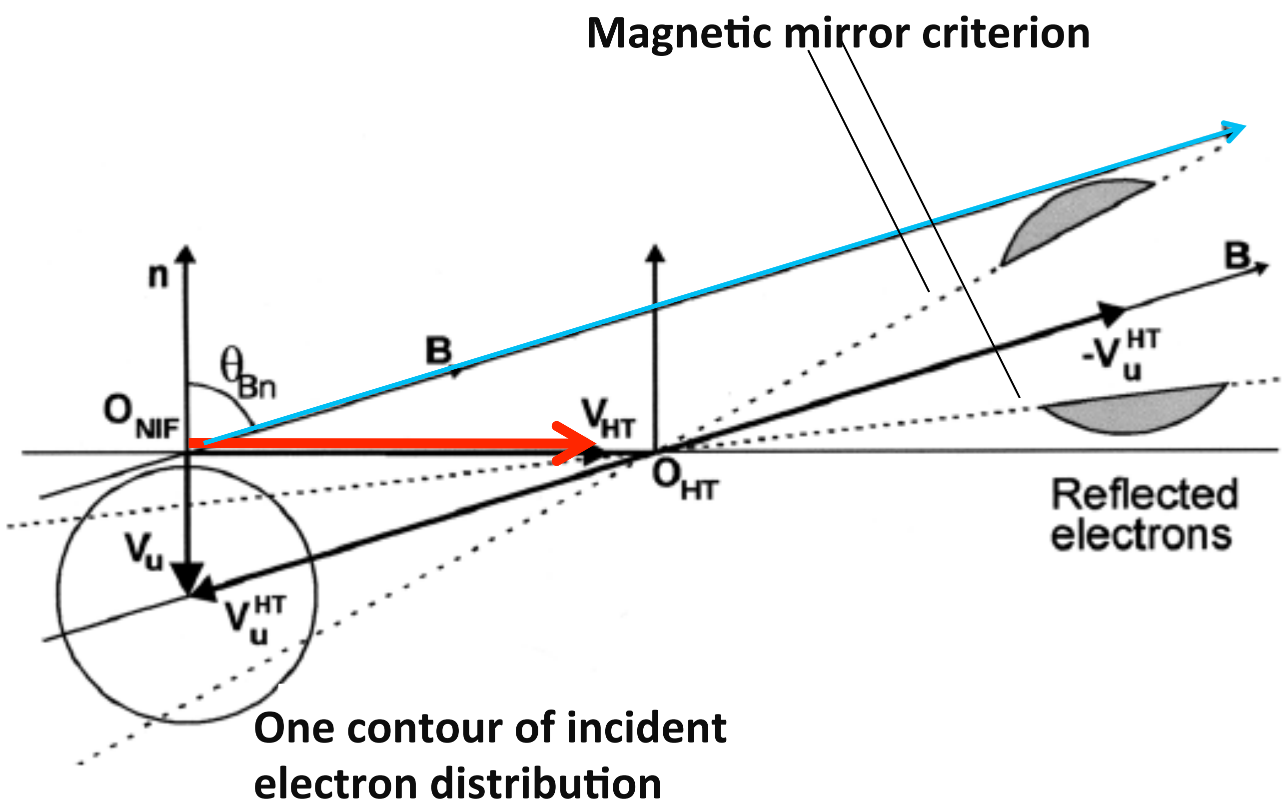

As V_{HT} increases (Θ_{Bn} closer to 90°) portion that mirrors comes increasingly from outer part of incident distribution: reflected density depends strongly on distribution function above thermal energies (non-Maxwellian tail).

Field –aligned beams (FABs) upstream of the quasi-perpendicular shock

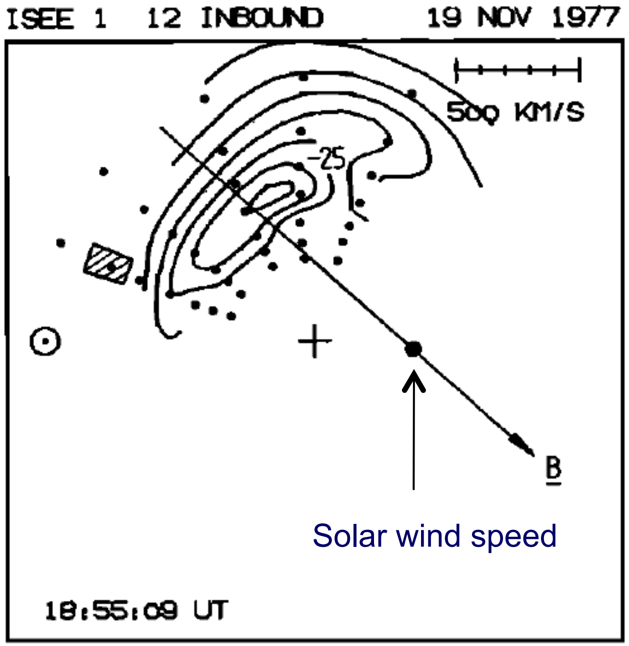

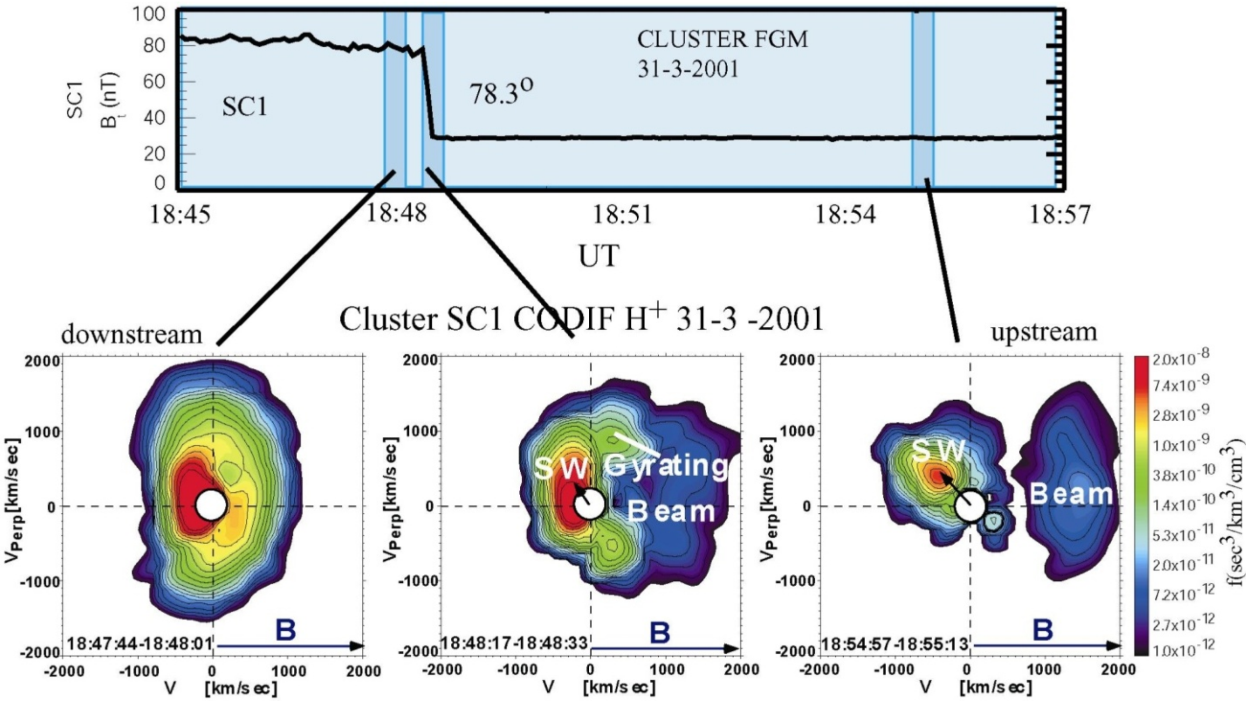

Paschmann et al. 1981

Kuchaek et al. 2004

SHOCK DRIFT ACCELERATION

Energy gain from motional electric field …

- if a particle can be held in shock frame
- and drifts in direction of electric field

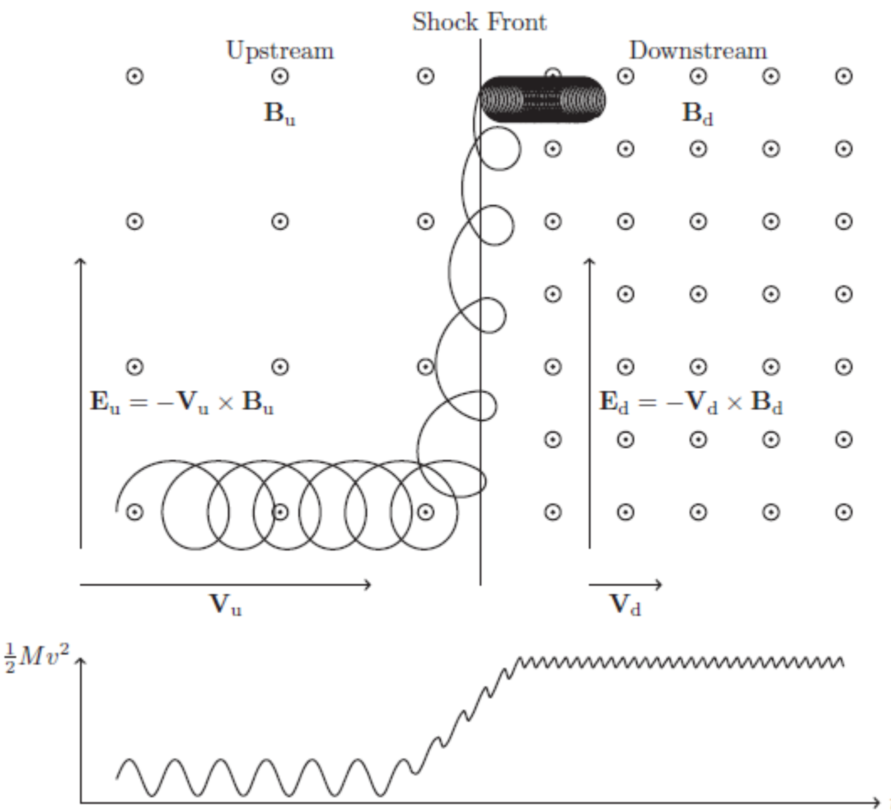

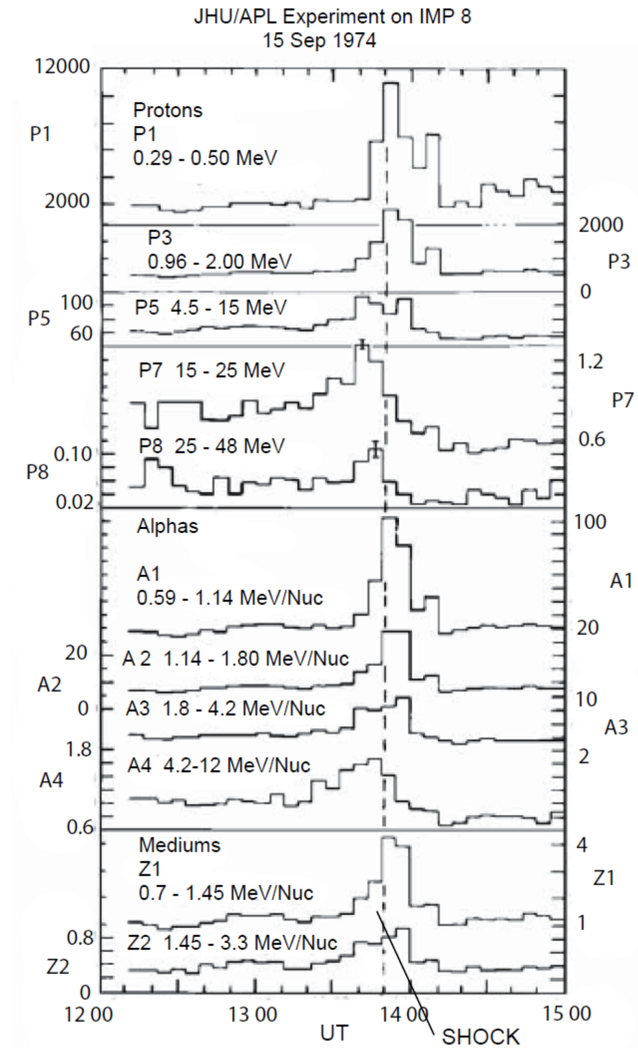

Diffuse ions upstream of Earh‘s quasi-parallel bow shock

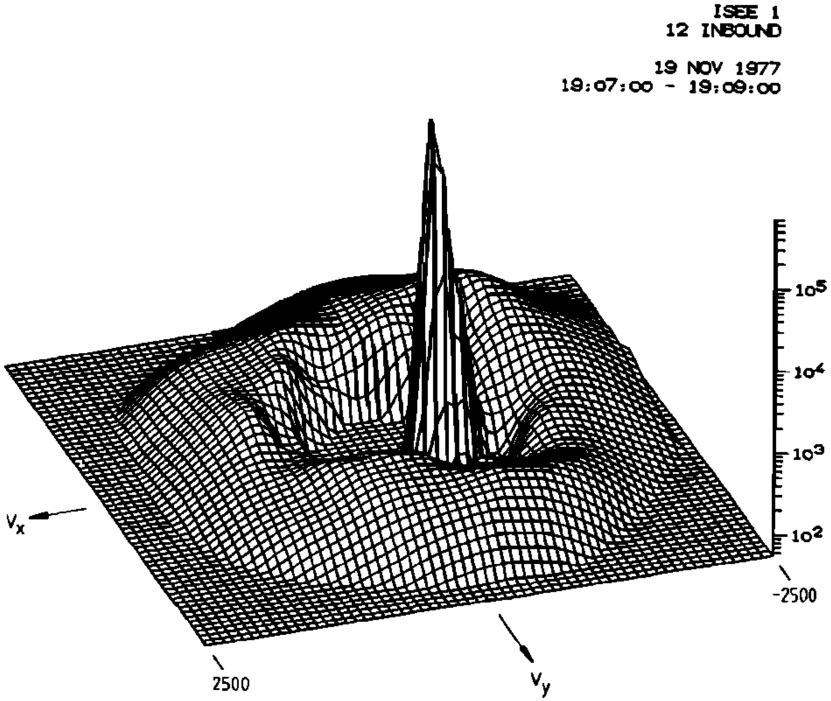

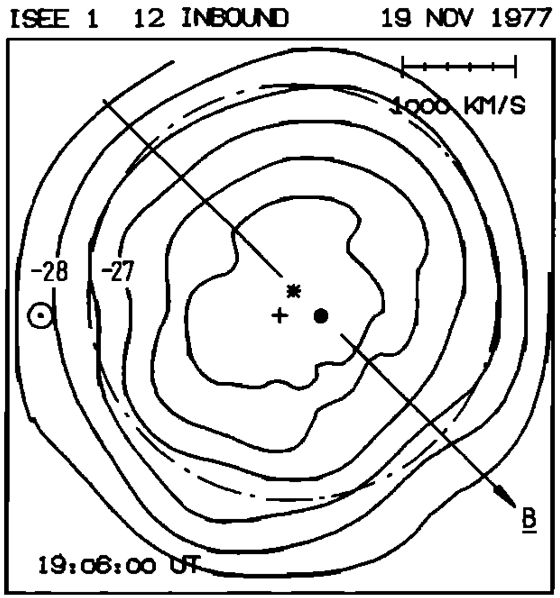

Paschmann et al. 1981

Diffuse Ion Spectra Upstream of Earth's Bow Shock

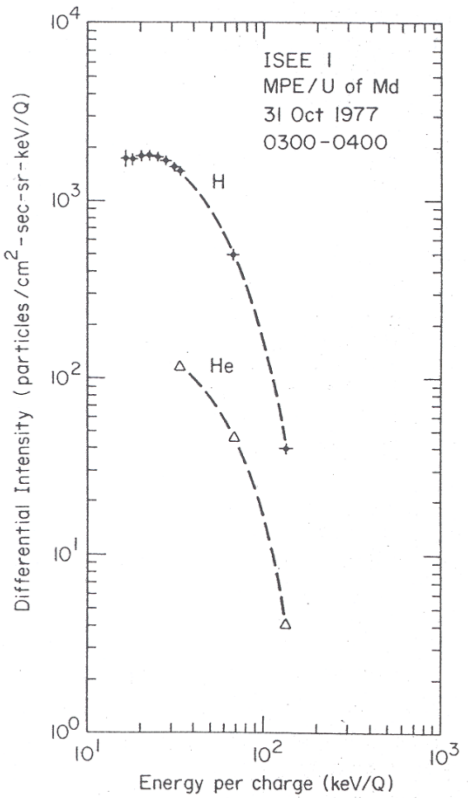

Log(flux) versus log(energy/charge)

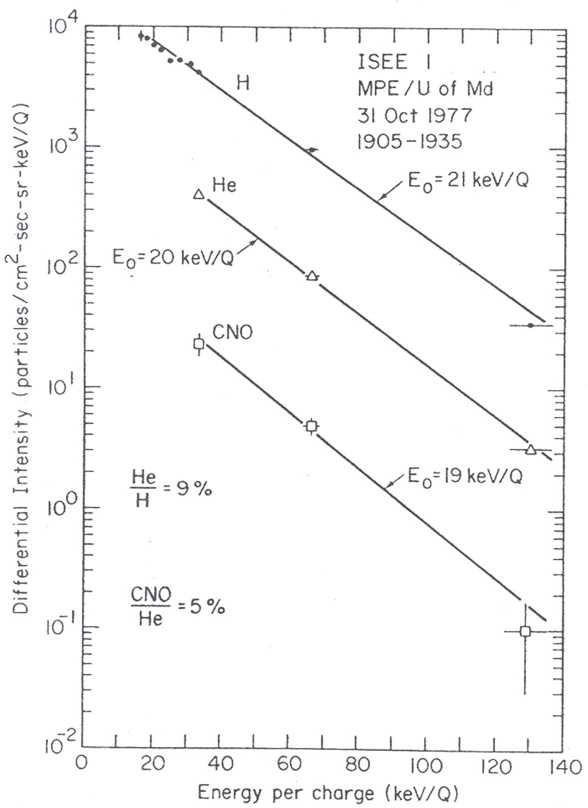

Log(flux) versus energy/charge (linear)

Spectra are exponentials in energy/charge with the same e-folding energy for all species

Ipavich et al. 1981

Cluster observations of diffuse upstream ions

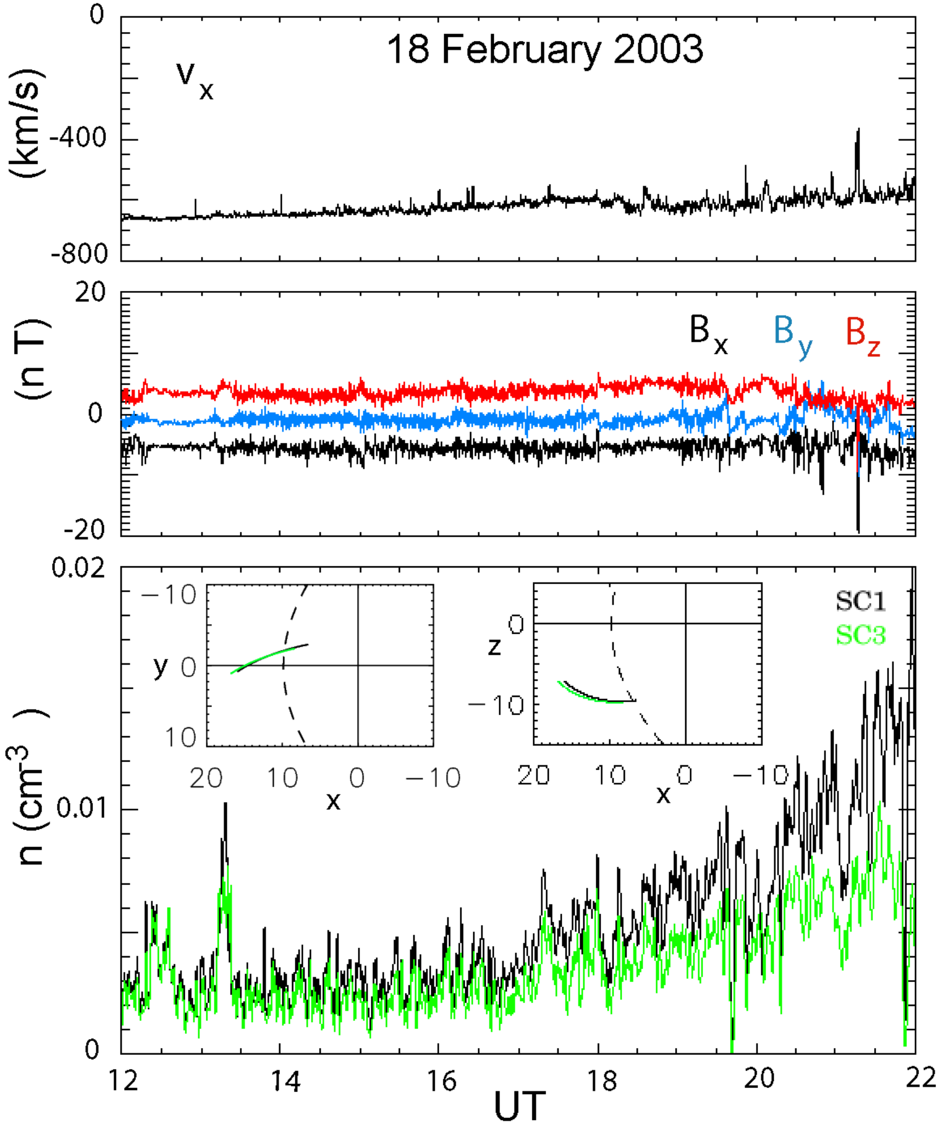

Particle density at 24 – 32 keV at two spacecraft, SC1 (black) and SC3 (green). SC3 was about 1.5 Re closer to the bow shock .

Kis et al. 2004

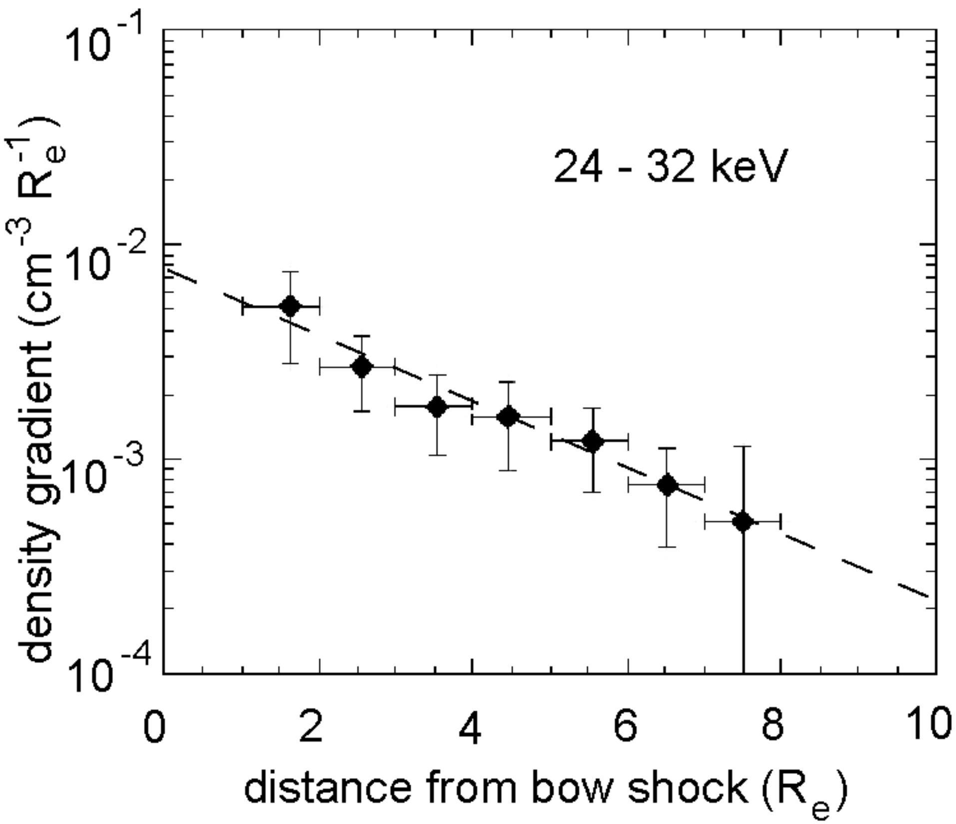

The gradient of upstream ion density in the energy range 24-32 keV as a function of distance from the bow shock (Cluster) in a lin vs log representation. The gradient (and thus the density itself) falls off exponentially.

Strong indication for diffusive transport in the upstream region:
Downstream convection is balanced by upstream diffusion

Diffusive Shock Acceleration

The Parker transport equation for energetic particles

1. Diffusion

2. Convection

3. Adiabatic decelation

The Parker transport equation for the phase space density f may be written as the sum of various physical effects, as indicated:

$$\frac{\partial f}{\partial t} = \frac{\partial}{\partial x_i}[\kappa_{ij}\frac{\partial f}{\partial x_j}] \qquad \text{(diffusion)}$$

$$-U_i\frac{\partial f}{\partial x_i} \qquad \text{(convection)}$$

$$+\frac{1}{3}\frac{\partial U_i}{\partial x_i}[\frac{\partial f}{\partial \ln p}] \qquad \text{(energy change)}$$

$$+Q(x_i, t, p) \qquad \text{(source term)}$$

This equation contains both spatial transport and acceleration. Statistical acceleration can be incorporated by adding momentum diffusion

$$\frac{1}{p^2}\frac{\partial}{\partial p}[p^2 D_{pp}\frac{\partial f}{\partial p}]$$

Consider a one-dimensional flow $U_x(x)$ as shown.

(the shock ratio $U_1 / U_2 < 4$)

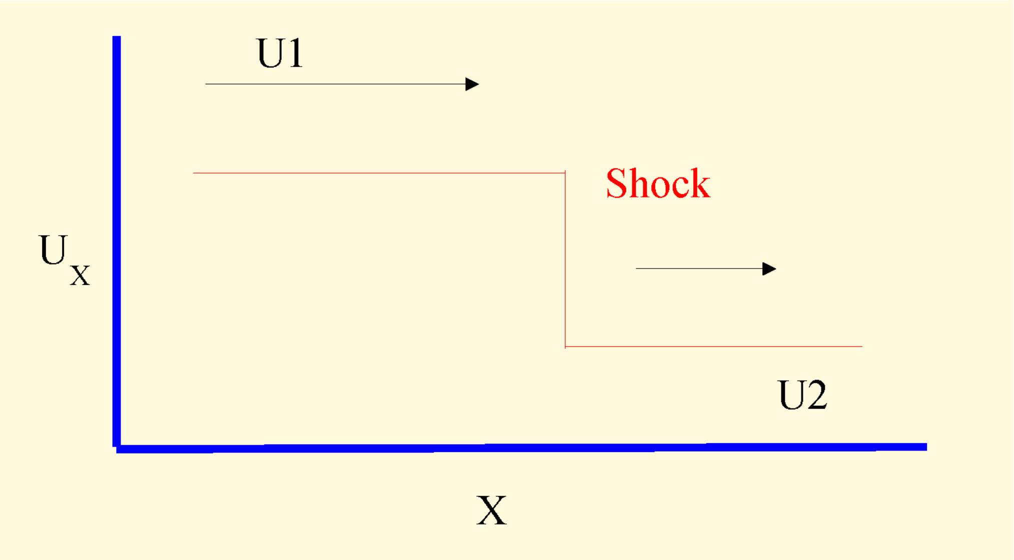

Solve the Parker transport equation for boundary condition

$$\frac{\partial U}{\partial x} = (U_2 - U_1)\delta(x)$$

$$f_1(x = 0) = f_2(x = 0)$$

For this system the steady state solution to Parker's equation for particles injected at momentum p_o has the characteristic form (above p_o):

$$\frac{dj}{dT} = p^2 f(x)$$

$$= Ap^{-q+2} \exp(\frac{U_1 x}{\kappa_{xx}}) \quad x < x_{shock}$$

$$= Ap^{-q+2} \quad x \geq x_{shock}$$

where $q = 3r/(r-1) \approx 4$ for strong shocks $\rightarrow$ $dj/dT \sim p^{-2} \approx T^{-2}$

Near-universal power law spectrum!

Solution of time-dependent Parker equation results in characteristic acceleration time for acceleration to to velocity v

(Laplace transform the Parker equation)

$$\tau_{acc} = \frac{3}{U_1 - U_2} \int^{v} \left(\frac{\kappa_{xx1}}{U_1} + \frac{\kappa_{xx2}}{U_2} \right) dv'$$

Earth's bow shock

Between L, diffusion coefficient , κ and solar wind velocity v_{sw} the following relation holds (stationary, planar shock):

$$L = \frac{\kappa_P}{v_{sw}}$$

Time scale for diffusive shock acceleration:

$$t_{acc} \approx \frac{3\kappa_{||}}{v_{sw}^2} = \frac{3L}{v_{sw}}$$

← e-folding distance

With L = 3 R_E at 30 keV and v_{sw} = 600 km/s one obtains:

t_{acc} = 120 s

The rate of increase in the cutoff momentum p_c depends on these parameters:

$$\frac{dp_c}{dt} \approx \frac{U_{sh}^2}{\kappa_{xx}}$$

1. Exponential rollover in energy spectrum above p_c

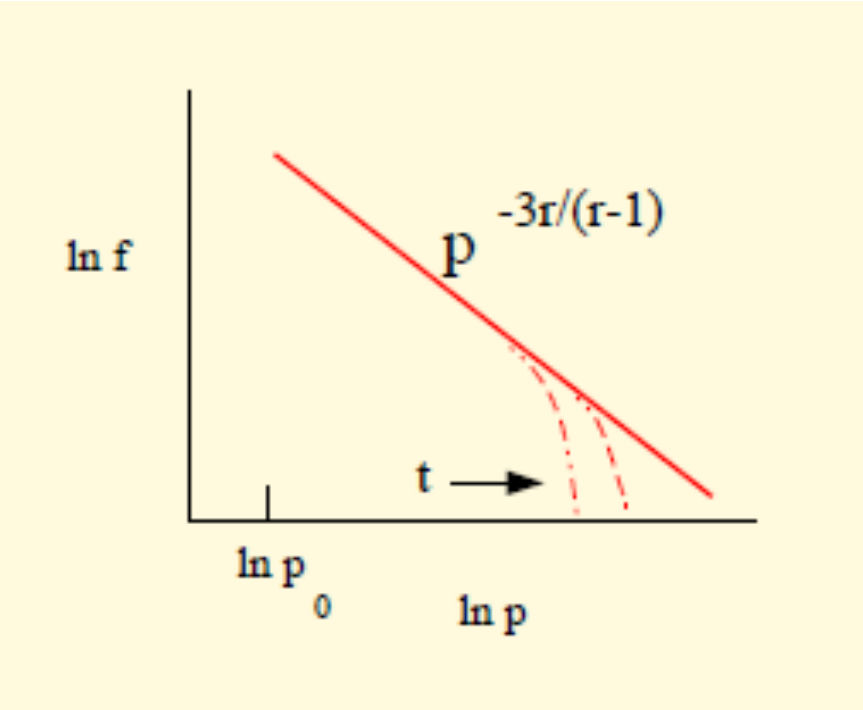

Simulating Diffusive Acceleration

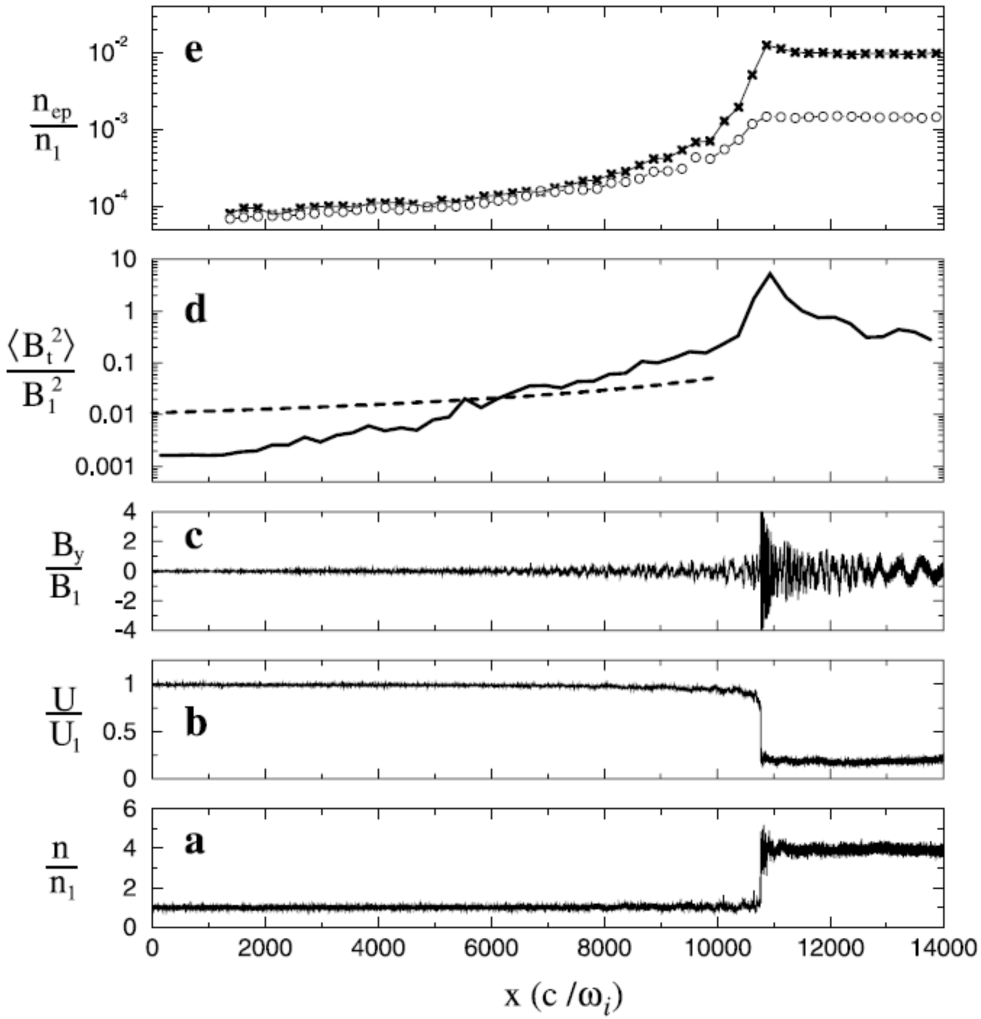

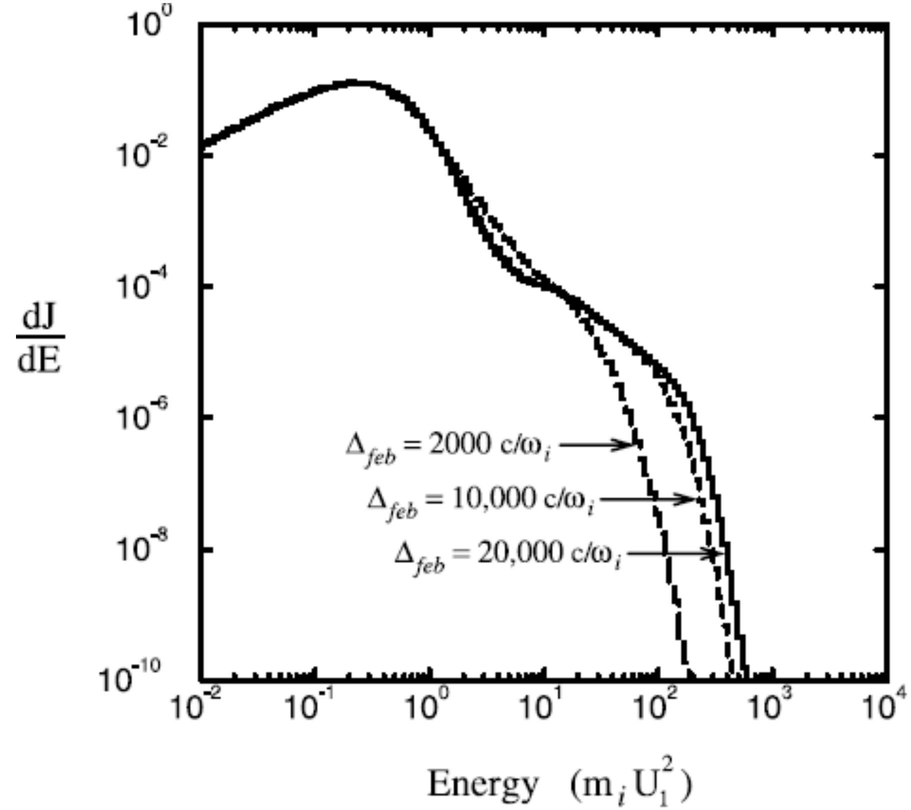

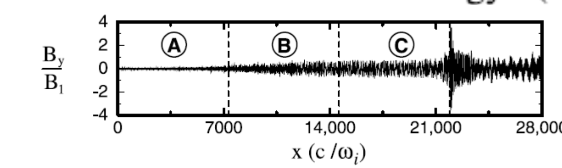

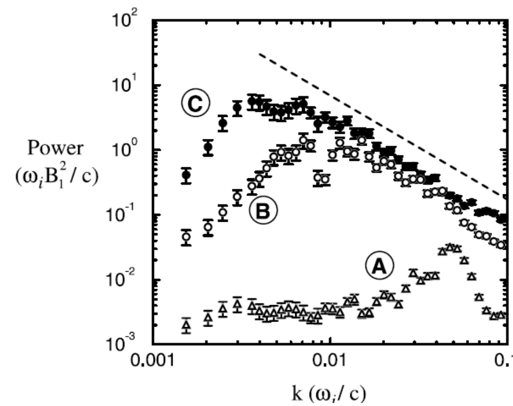

Giacalone 2004

Simulating Diffusive Acceleration

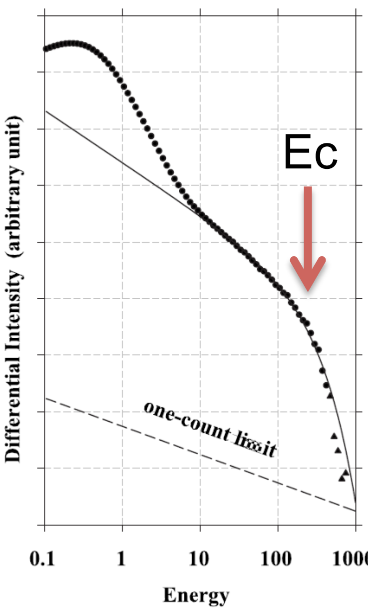

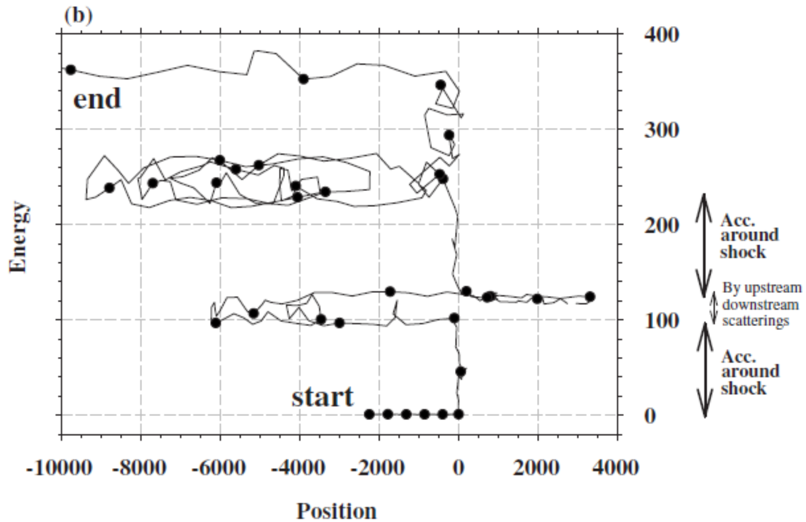

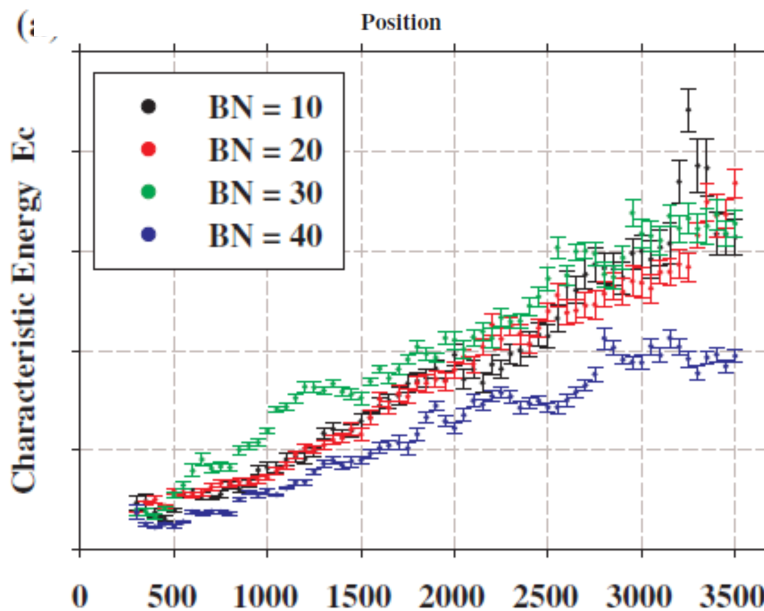

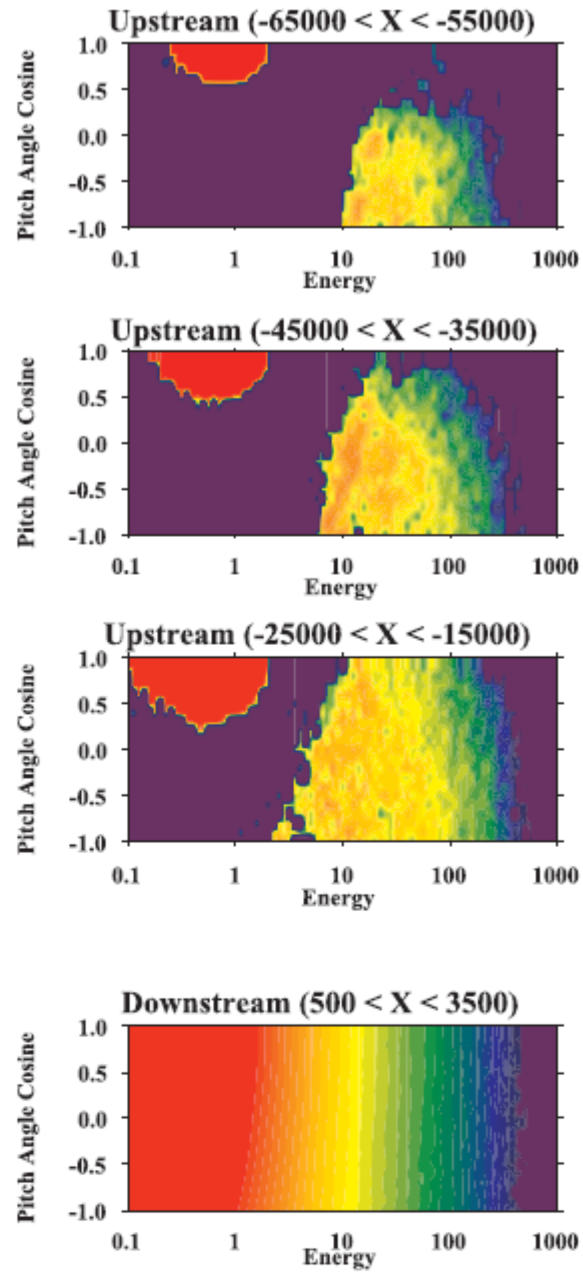

Sugiyama 2011

INTERPLANETARY SHOCKS AND PARTICLE ACCELERATION

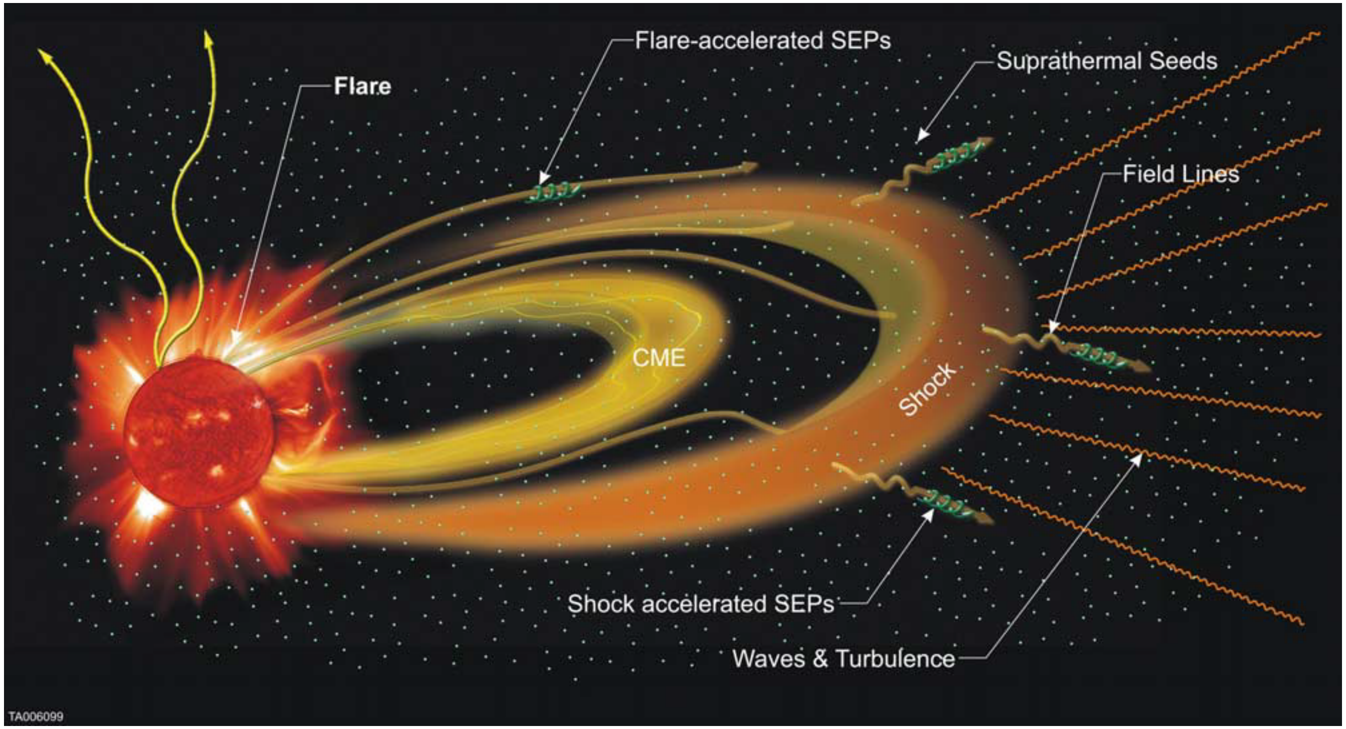

Desai 2008

INTERPLANETARY SHOCKS AND PARTICLE ACCELERATION

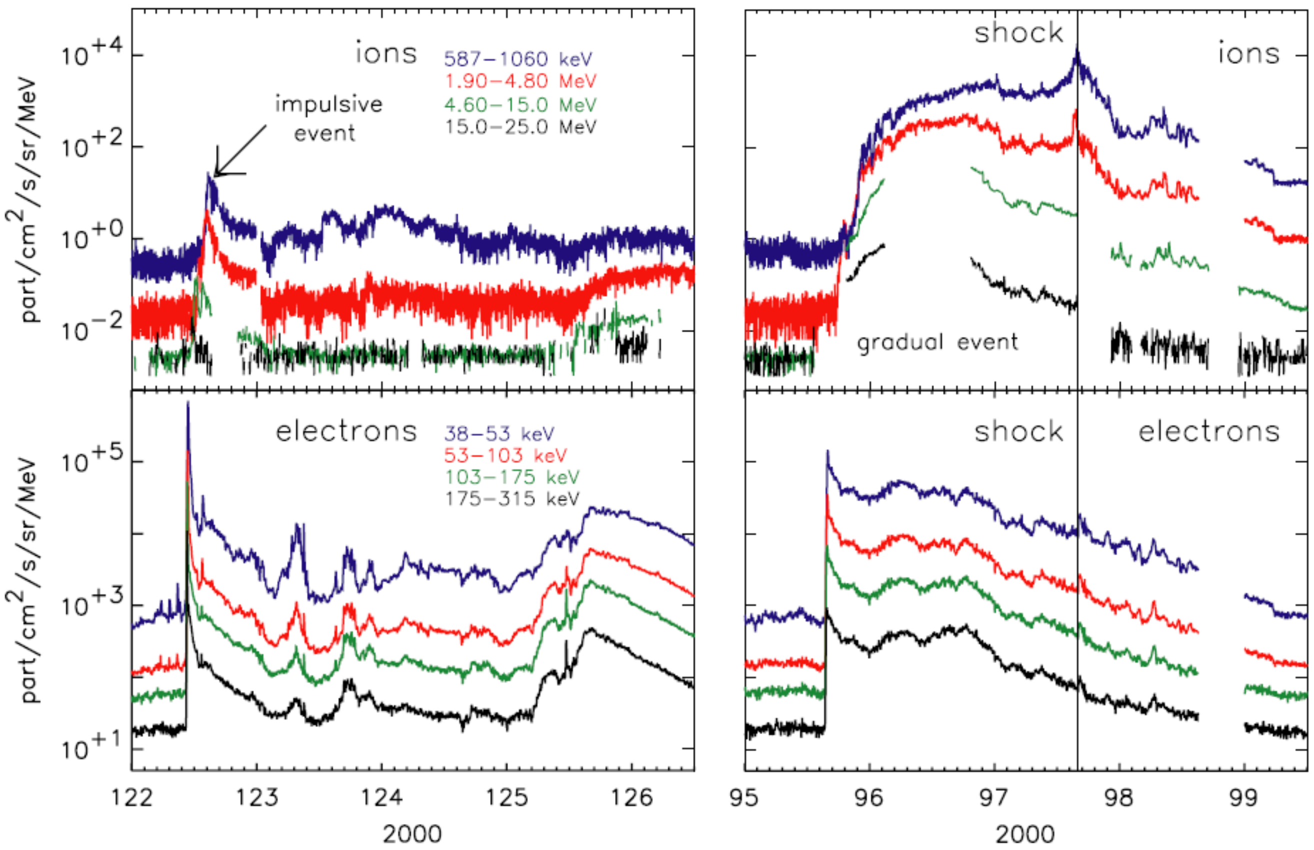

Lario 2005

INTERPLANETARY SHOCKS AND PARTICLE ACCELERATION

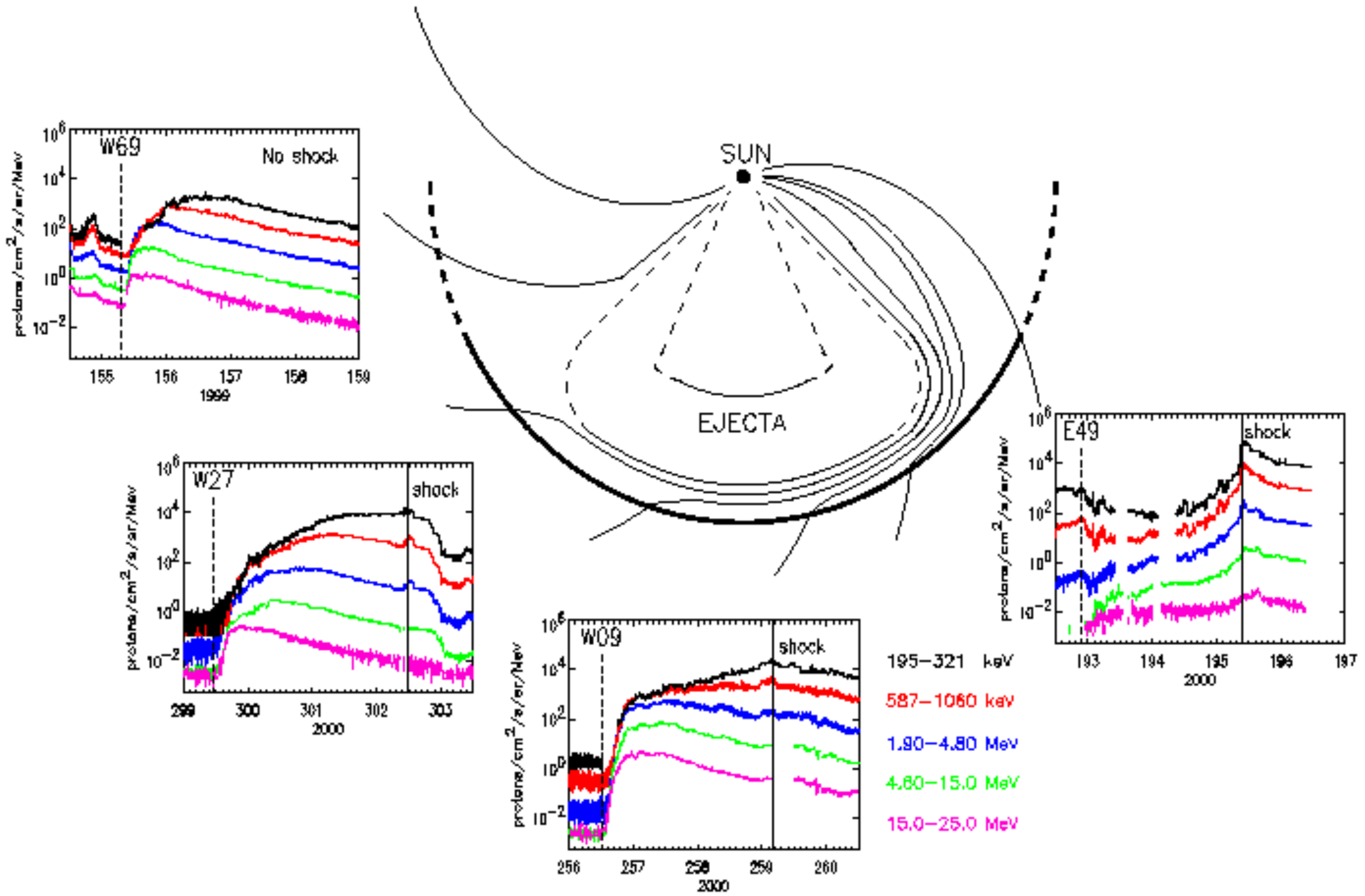

Lario 2005

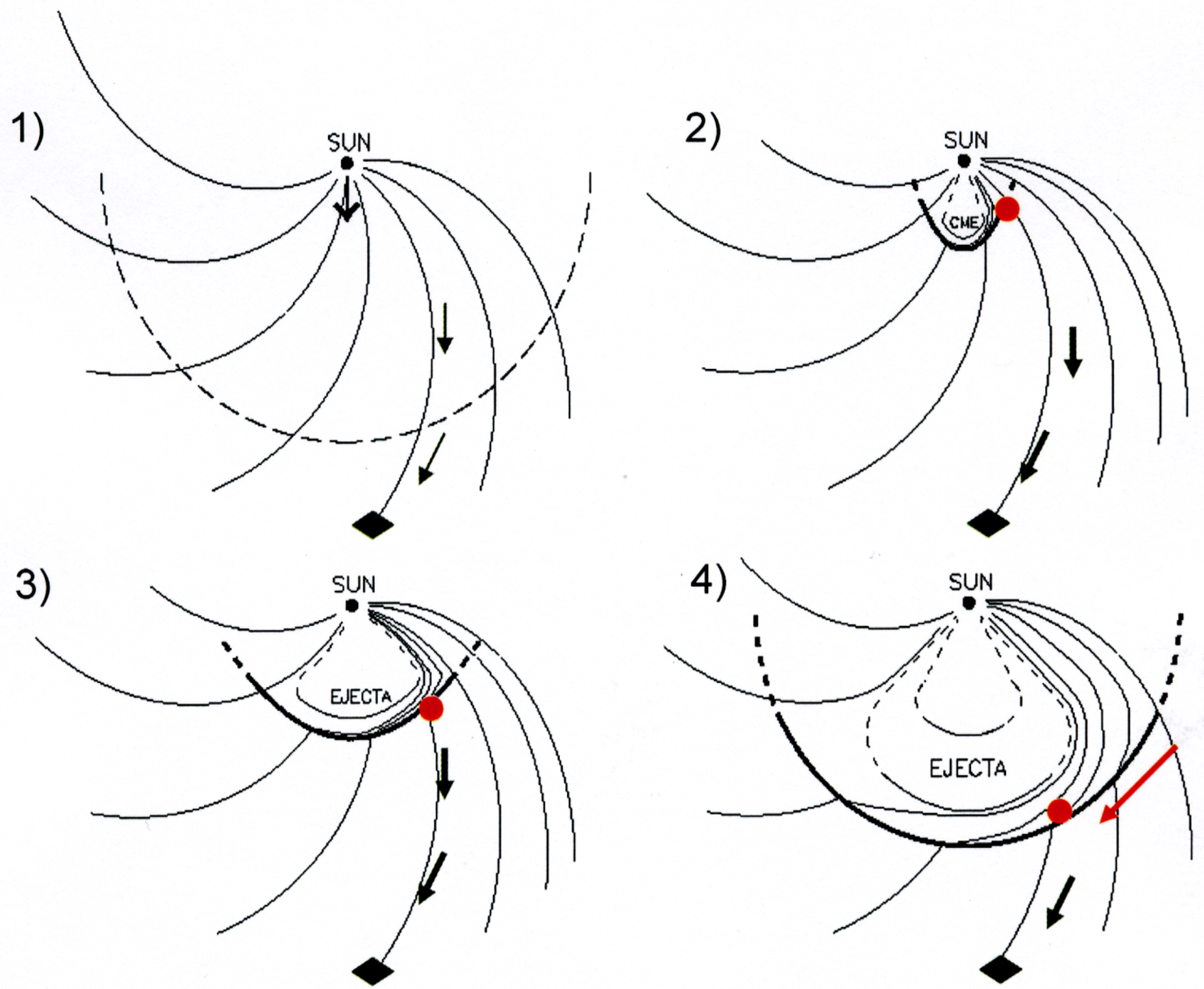

Aran 2007

MODELING PARTICLE ACCELERATION FOR SOLAR ENERGETIC PARTICLE EVENTS

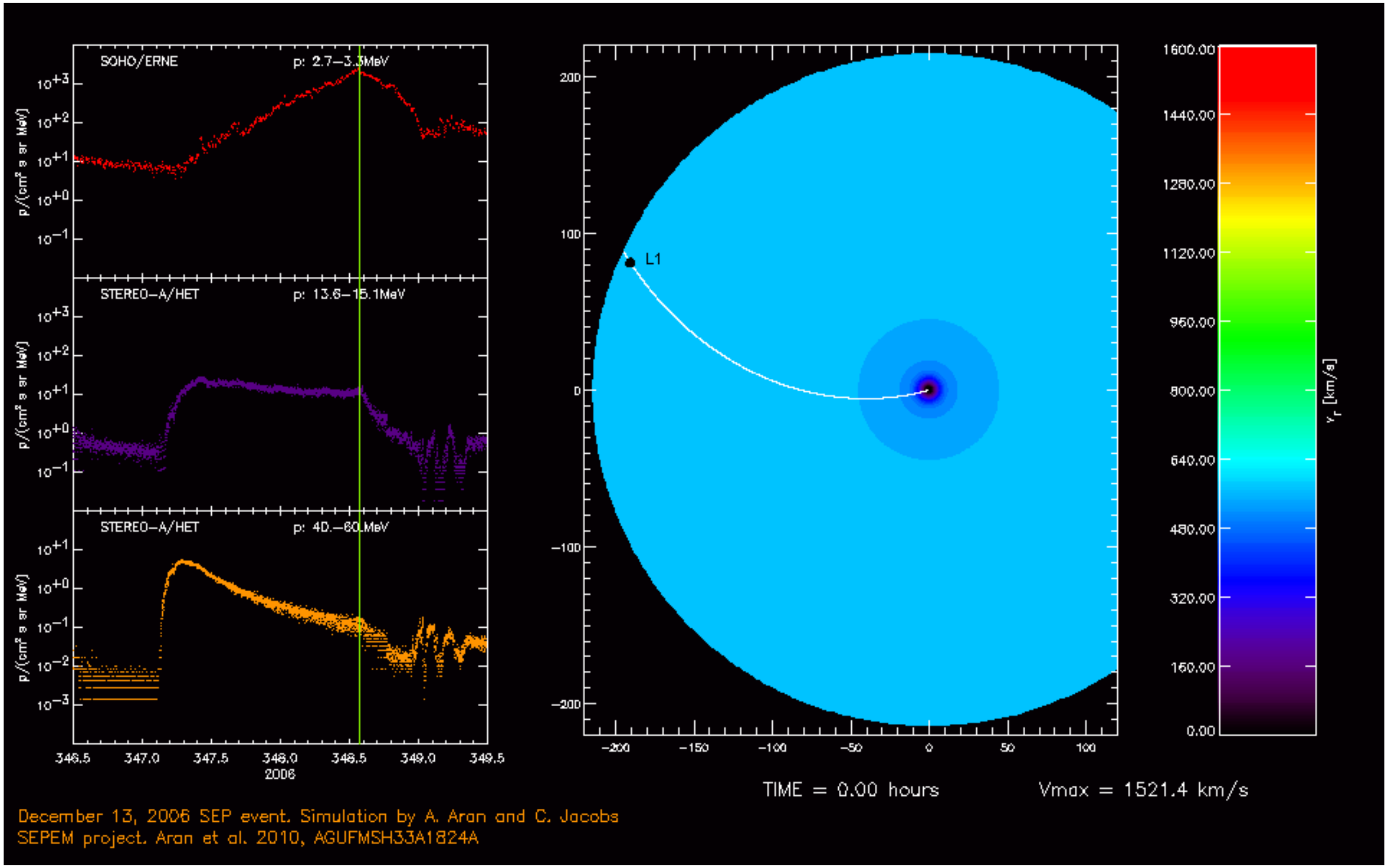

Aran A., N. Agueda, C. Jacobs et al. 2011, AGU, Fall Meeting 2011, abstract **#SH33B-2051A**.

Thank you!